ACS NANO

www.acsnano.org

REVIEW

# Alignment of Cellulose Nanofibers: Harnessing Nanoscale Properties to Macroscale Benefits

Kai Li,* Caitlyn M. Clarkson, Lu Wang, Yu Liu, Meghan Lamm, Zhenqian Pang, Yubing Zhou, Ji Qian, Mehdi Tajvidi, Douglas J. Gardner, Halil Tekinalp, Liangbing Hu, Teng Li, Arthur J. Ragauskas, Jeffrey P Youngblood, and Soydan Ozcan*

Cite This: *ACS Nano* 2021, 15, 3646–3673

Read Online

ACCESS | Metrics & More | Article Recommendations

**ABSTRACT:** In nature, cellulose nanofibers form hierarchical structures across multiple length scales to achieve high-performance properties and different functionalities. Cellulose nanofibers, which are separated from plants or synthesized biologically, are being extensively investigated and processed into different materials owing to their good properties. The alignment of cellulose nanofibers is reported to significantly influence the performance of cellulose nanofiber-based materials. The alignment of cellulose nanofibers can bridge the nanoscale and macroscale, bringing enhanced nanoscale properties to high-performance macroscale materials. However, compared with extensive reviews on the alignment of cellulose nanocrystals, reviews focusing on cellulose nanofibers are seldom reported, possibly because of the challenge of aligning cellulose nanofibers. In this review, the alignment of cellulose nanofibers, including cellulose nanofibrils and bacterial cellulose, is extensively discussed from different aspects of the driving force, evaluation, strategies, properties, and applications. Future perspectives on challenges and opportunities in cellulose nanofiber alignment are also briefly highlighted.

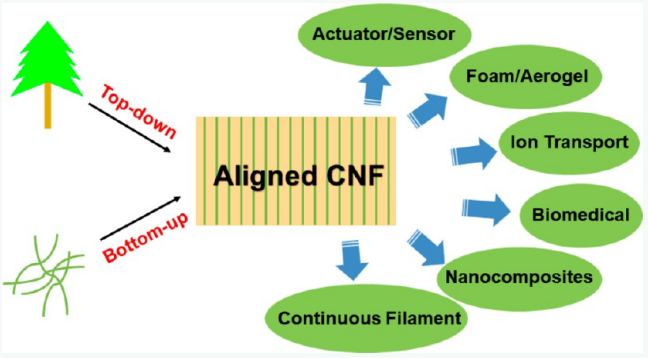


**KEYWORDS:** *nanocellulose, cellulose nanofibrils, cellulose nanofiber, fiber alignment, bacterial cellulose, functional materials, anisotropic properties, nanocellulose self-assembly*

Various living organisms in nature use nanoscale components to construct hierarchical structures to achieve high-performance properties and different functionalities.[1,2] These nanoscale components are well assembled and fully exploit the material characteristics of each component. In wood and other plants, repeating $\beta$-(1,4)-linked D-glucose units form cellulose polymer chains and assemble into semi-crystalline structures (2–5 nm) with disordered and crystalline regions. These semi-crystalline structures further assemble with disordered components into nanofibrils, which have a diameter ranging from 20 to 100 nm. The nanofibrils are mainly oriented along the longitudinal direction of the cell and further form 2D laminar or 3D helicoidal structures. These 2D laminar structures combine with lignin and hemicellulose to form the cell wall in plants. This complicated hierarchical structure assembles across multiple length scales and helps impart exceptional mechanical properties to wood.

Cellulose nanomaterials (CNMs) can be separated from plant or animal tissues using mechanical fibrillation combined with chemical or biological treatment.[3−5] These separated structures include cellulose nanocrystals (CNCs, also referred to as "cellulose nanowhiskers" or "nanocrystalline cellulose") and cellulose nanofibrils (CNFs; sometimes, micro- or nanofibrillated cellulose is also used). CNCs are rigid, rod-shaped particles with dimensions of 100–200 nm long and 5–

Received: September 9, 2020
Accepted: January 21, 2021
Published: February 18, 2021







https://dx.doi.org/10.1021/acsnano.0c07613
*ACS Nano* 2021, 15, 3646–3673

20 nm wide.[4] CNFs are fibril structures with a length of >1 μm and width of 5−200 nm.[4] CNCs and CNFs are mainly isolated from plants, such as wood and bamboo, but can also be obtained from some animal tissues, such as tunicates.[4] In addition to CNCs and CNFs, bacterial cellulose (BC) generated by bacteria such as *Acetobacter xylinum* through biosynthesis also represents an important type of CNMs. BC has a length up to several micrometers and width around 25−86 nm.[5]

CNMs have received significant attention in recent years owing to their good properties, including sustainability, light weight, and high mechanical properties.[6−12] CNMs can be processed into multiple architectures, such as films, fibers, aerogels, and hydrogels, which has led to the investigation of these materials for various applications.[6−12] Studies have shown that the performance (*e.g.*, mechanical properties) of macroscale nanocellulose materials, including their toughness and strength, highly depends on the degree of the cellulose nanofiber alignment.[13−16] Meanwhile, inspired by the assembly behavior of cellulose nanofibers in nature, researchers are also trying to mimic the assembly process to achieve the desired properties that exist in nature. The goal of aligning nanocellulose is to impart the excellent nanoscale properties, such as stiffness and strength, to a macroscale material.

In this review, the alignment of the cellulose nanofibers, including CNFs and BC, is extensively reviewed. First, the driving forces and evaluation of cellulose nanofiber alignment are discussed. Second, strategies to induce cellulose nanofiber alignment are summarized based on bottom-up and top-down methodologies. Third, different applications of aligned cellulose nanofibers are reviewed. Finally, future perspectives and concluding remarks are given. Alignment of CNCs is not included in this review, because it has been extensively reviewed by different researchers,[15−17] whereas the alignment and self-assembly behavior of CNFs and BC have received less attention. Compared with CNCs, aligning of CNFs and BC is much more challenging because of their long length and fiber network formation (or entanglement). Additionally, as reported in some literature,[18−21] microfibrillated cellulose (MFC) or cellulose microfibers are used. As long as one dimension is within the nanometer scale and it has fibrous structure, we included in this review.

## WHY ARE ALIGNED CELLULOSE NANOFIBERS NEEDED?

The alignment of cellulose nanofibers is important for nanocellulose-based materials. The driving forces behind these efforts are to allow for control of the macroscale properties. Here, we illustrate some of the motivations for pursuing aligned CNFs and BC, including the need for *anisotropic properties*; balancing stiffness and strength in *structural materials*; maximizing reinforcement efficiency in *fiber-reinforced composites*; and advancements in *biomaterials*. Of course, there are some other factors that drive the efforts to align cellulose nanofibers to achieve better performance. The overall motive behind these efforts is to achieve the optimal macroscale performance that can fully exploit the excellent properties of cellulose nanofibers.

**Anisotropic Properties.** Anisotropic properties exist in many materials, such as anisotropic optical properties of liquid crystals,[22] anisotropic conductivity of carbon nanotubes (CNTs),[23] and anisotropic mechanical properties of wood,[24] and have been used in materials design. Numerous efforts to make cellulose nanofiber-based materials through control of the alignment to realize anisotropic properties in macroscopic materials have been reported. Hu *et al.* developed a transparent cellulose nanofiber-based film through aligning cellulose nanofibers with anisotropic mechanical properties.[25] Moreover, these anisotropic films could provide a substrate for liquid spreading preferentially in the cellulose nanofiber-oriented direction. Another example is cellulose nanofiber-based heat-spreading substrate materials for effective cooling in paper electronics, to help avoid thermal failure.[26] One challenge is the development of heat-spreading substrates with in-plane anisotropic thermal conductivity. Research efforts have shown that in-plane anisotropic thermal conductivity of nanopaper could be realized by controlling the alignment of cellulose nanofibers.[27,28] Additionally, other interesting nanocellulose fiber-based materials with anisotropic properties have also been developed, such as paper-based sensors,[29] hydrogels,[30,31] and aerogels.[32]

**Structural Materials.** The elastic moduli of highly crystalline fibrils are around 150 and 18−50 GPa in the longitudinal and transverse directions, respectively.[33−35] However, the macroscale materials made from CNFs, such as film and filaments, are not as stiff as the nanoscale fibers,[33,36] leaving unmatched potential compared with individual CNFs. Various strategies have been developed to improve the mechanical properties of these CNF-based materials; one promising strategy is to preferentially align CNFs along a preferential direction in the bulk materials. Bulk cellulose fiber made from highly aligned CNFs can be as strong as glass fiber and as stiff as Kevlar in the fiber alignment direction.[37,38] However, the strength in the direction perpendicular to the alignment is relatively lower compared to that in the parallel direction, and the tear strength is poor,[39,40] due to the anisotropic elastic properties of cellulose fibers.[41] This can be solved by stacking the aligned fibers together in preferential directions to achieve high strength in different directions.[42] Through utilizing the highly aligned CNFs in wood, Hu *et al.* demonstrated a "superwood" to be used as a potential lightweight structural material.[42] This material achieved a specific strength of 451 MPa $cm^{-3}$ $g^{-1}$, which is much higher than that of structural metals and alloys. One challenge for structural materials is how to achieve high strength and toughness at the same time.[43] In general, tough materials are not strong, and strong materials are not tough. However, in nature, many tough and stiff materials exist through formation of complicated hierarchical structures, such as nacre.[44] Some efforts on the assembly of CNFs into hierarchical structures to mimic natural materials have yielded strong and tough materials. For instance, strong and tough cellulose macrofibers were developed by aligning CNFs during the spinning process with the assistance of magnetic/electric fields or mechanical stretching.[13,45] Geng *et al.* also reported very strong and tough nanocomposites reinforced by aligned poly(ethylene glycol) (PEG)-modified CNFs.[46] Therefore, effective alignment of CNFs in the macroscale materials could achieve strong and stiff structural materials.

**Fiber-Reinforced Composites.** Cellulose nanofibers are stiff, have a high aspect ratio, are abundantly available, are renewable, and are good for polymer composites reinforcement to achieve high mechanical performance.[3,4,47−49] For cellulose nanofiber-reinforced composites, dispersion and interfacial adhesion are primary concerns.[50] Additionally, the orientation or alignment of the cellulose nanofibers signifi-


https://dx.doi.org/10.1021/acsnano.0c07613
ACS Nano 2021, 15, 3646−3673

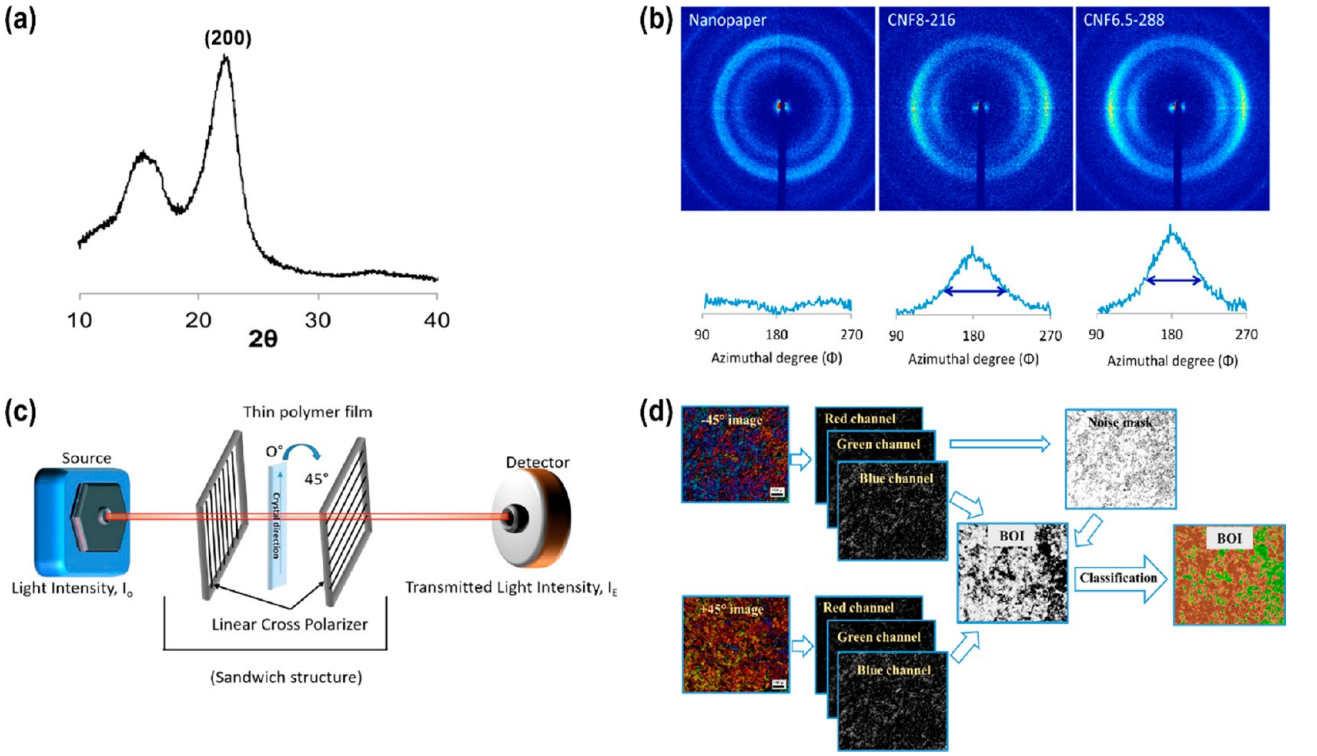


**Figure 1. (a) XRD diffractograms of cellulose nanofiber. (b) WAXS patterns of CNF-based materials. Adapted with permission from ref 61. Copyright 2015 American Chemical Society. (c) Schematic representation of the birefringence technique. Adapted with permission from ref 79. Copyright 2017 Springer Nature. (d) The process to produce the orientation index map using BOI. Reused with permission from ref 81. Copyright 2019 Springer Nature.**

cantly influences the performance of the composites, similar to most fiber-reinforced composites. However, fiber alignment in polymer composites is not yet fully realized. The orientation of cellulose nanofibers in polymer materials is scientifically and technically challenging. Stretching-induced alignment of BC could significantly improve the mechanical properties of BC−soy protein composites by 275% in tensile strength and 300% in tensile modulus compared with randomly oriented BC.[51] Similarly, improvement in composite mechanical properties by aligning CNFs has also been observed in other studies.[52−54]

**Biomaterials.** Cell alignment exists widely in tissues and organs, such as extracellular matrices (ECMs) in tendons and bones.[55,56] How to *in vitro* engineer cell alignment is one of the essential research topics for biomedical applications.[57] Cells are usually cultured *in vitro* on substrates, and the morphology of the substrates strongly influences the cell adhesion and orientation, since cells can replicate the morphology of the substrate. Different patterning methods have been developed to create patterned substrates for cell culture.[58] The importance of the substrate's pattern in cell culture originates from the significance of cell alignment,[57] which is critical in various cell behaviors, such as ECM remodeling, cytoskeleton reorganization, and tissue regeneration. One strategy to engineer the cell alignment is topographical patterning, which uses patterns on the substrate (*e.g.*, fibrous scaffolds) to align cells.[57] Tseng *et al.* utilized an electrospun fibrous substrate to regulate cell alignment and found that cells preferentially aligned along the direction of the scaffold fiber alignment.[59] Cellulosic nanomaterials are biocompatible and have high water retention capabilities,[60] which are desirable qualities in biomaterial applications (*i.e.*, substrates for cell growth). Therefore, the alignment of CNFs is important for the use of CNFs in biomaterials.

## ALIGNMENT EVALUATION

Different methodologies have been used for evaluating the alignment of cellulose nanofibers, such as scanning electron microscopy (SEM),[61−64] atomic force microscopy (AFM),[65] Raman spectroscopy,[66,67] polarized optical microscopy (POM),[68] small- and wide-angle X-ray scattering (SAXS and WAXS),[69,70] and birefringence measurement.[71] Both qualitative and quantitative means have been applied to evaluate the alignment of cellulose nanofibers formed from various processes. In most cases, a combination of qualitative and quantitative analyses is used for a scientifically sound discussion of the alignment process. Here, some widely used strategies are discussed. Readers interested in gaining a deeper understanding of the characterization of CNMs are referred to an extensive review by Foster *et al.*[72]

X-ray scattering, including SAXS and WAXS, is most commonly used to evaluate the fiber alignment quantitatively.[45,61,62,73−75] An orientation index ($f_c$) calculated from X-ray scattering data is widely accepted to quantify the fiber alignment. The principles of SAXS and WAXS can be found in other sources.[76] Samples are first scanned by X-rays perpendicularly at a chosen angle range to yield a diffraction pattern. The diffraction pattern shows the crystallographic lattice planes of the sample. The angle, corresponding to the lattice plane of highest diffraction intensity, is often selected for a second scan, referred to as an azimuthal scan. For cellulose, the lattice plane of (200) (Figure 1a) is widely used for the azimuthal scan. The azimuthal scan checks the sample in parallel at 360° to produce diffraction patterns (Figure 1b),


https://dx.doi.org/10.1021/acsnano.0c07613
ACS Nano 2021, 15, 3646−3673

which are integrated to generate a distribution of diffraction intensity ($I(\Phi)$) vs azimuthal angle ($\Phi$) for quantifying the alignment of the fibers. The ordered parameters ($S$) can be calculated using the following equations:[77,78]

$$f_c = \frac{180^\circ - \text{fwhm}}{180^\circ} \quad (1)$$

$$S = \frac{3\cos^2 \Phi_{c,z} - 1}{2} \quad (2)$$

$$\cos^2 \Phi_{c,z} = 1 - 2\cos^2 \Phi_{200,z} \quad (3)$$

$$\cos^2 \Phi_{200,z} = \frac{\sum_0^\pi I(\Phi) \sin \Phi \cos^2 \Phi}{\sum_0^\pi I(\Phi) \sin \Phi} \quad (4)$$

where $f_c$ is the orientation index, fwhm is the full width of the half-maximum of the azimuthal profiles from the selected equatorial reflection, $S$ is the Herman's order parameter, $\Phi$ is the azimuthal angle, and $I(\Phi)$ is the intensity distribution along the Debye−Scherrer ring. A value of $S = 0$ means the cellulose fiber is randomly oriented, while $S = 1$ indicates a full fiber alignment.

Birefringence from optical anisotropy and refractive index differences can also be used to calculate the degree of the fiber alignment. Birefringence captured by POM offers a cost-effective, quantitative way of evaluating fiber alignment when combined with image processing software, such as ImageJ.[79,80] The fiber is placed between linear cross polarizers and rotated to identify the position with minimum light intensity (Figure 1c). Such a location is taken as 0°. The maximum light intensity of the fiber should appear by rotating the fiber 45°. Both micrographs at the dark field of 0° and bright field of 45° are taken and loaded into ImageJ software to extract pixel intensity of the background and the fiber. Besides being simple and inexpensive, authors claim the birefringence method is a more accurate measurement of the order parameter because it considers both the crystalline and disordered contributions to the measured fiber orientation, rather than just the crystalline contribution determined by the WAXS method.[79,80] Similarly, Ghasemi *et al.* developed the birefringence orientation index (BOI) (Figure 1d) based on the interference color changes between two angles (+45° and −45°) to map the fibril orientation in CNF films.[81] The proposed BOI values range between −1 and +1, differentiating orientation in perpendicular directions. The results suggested that the BOI works successfully for CNF films and is also applicable in the measurement of polymer chain orientation in polyvinyl chloride films.

## STRATEGIES TO ALIGN CELLULOSE NANOFIBERS

The properties achieved in cellulose nanofiber bulk materials by tuning the alignment of cellulose nanofibers lead to the development of different strategies, including bottom-up and top-down strategies, to align cellulose nanofibers. Bottom-up strategies align cellulose nanofibers by assembling nanoscale fibrils into ordered macroscale materials. The bottom-up strategy provides tunability of the cellulose nanofiber alignment and can control the hierarchical structure in the macroscale materials. Bottom-up strategies include magnetic and electric fields, liquid state shear and extensional methods, drawing processes, templating effects, and spinning, or a combination of them. These strategies will be discussed separately in this review. Contrary to the bottom-up strategy that starts from the nanoscale fiber, the top-down strategy directly utilizes the hierarchical structure of a plant, such as wood, where CNFs are already well aligned by plant growth. The top-down strategy usually requires chemical treatments to partially or fully remove lignin and hemicellulose.[82] Top-down strategies provide a well-aligned CNF structure in bulk materials. Both bottom-up and top-down strategies have been extensively investigated to achieve high-performance materials. Table 1 summarizes some examples of both strategies.

## BOTTOM-UP STRATEGIES TO ALIGN CELLULOSE NANOFIBERS

**Magnetic and Electric Alignment of Cellulose Nanofibers.** *Magnetic Field Alignment.* Diamagnetic fibers with magnetic anisotropy can be aligned in strong magnetic fields, if they are suspended in a medium that allows non-restricted alignment.[19] The direction of such alignment depends on the nature of the magnetic anisotropy of the fibers; for fibers with positive diamagnetic anisotropy, the alignment will be along the magnetic field direction, whereas fibers with negative diamagnetic anisotropy, such as CNFs, will align in the plane perpendicular to the magnetic field direction.[19] If the alignment is obtained on a 2D substrate, the rotation of fibers will be limited by the substrate, leading to unidirectional alignment perpendicular to the magnetic field direction.[84] Kim *et al.* evaluated the alignment performance of CNFs produced from cotton using a strong magnetic field of 5.3 T and reported that alignment of CNFs was achieved after 180 min.[83]

Magnetically aligning cellulosic fibers is achievable at various fiber size scales from millimeters (pulp fibers) to nanometers.[84] For larger pulp fibers that are naturally twisted and bent, a relatively good alignment can be achieved but even the strongest magnetic fields applied are unable to fully stretch the fibers. The alignment needs to be maintained once achieved. This can be done by simply evaporating the suspending medium (mostly water) or replacing the medium with a curable (usually UV-curable) resin that can cure after alignment is achieved to fix the fiber orientation in the desired direction. Both static and rotational magnetic fields can be used for cellulose fiber alignment, with rotational magnetic fields usually yielding better results.[19,84]

A high magnetic field strength is required (up to 20 T) to orient diamagnetic cellulosic fibers.[100] Efforts have been made to deposit superparamagnetic magnetite particles on the surface of wood pulp and then align them using regular low-strength magnets (0.18 T strength).[100] The concentration of magnetic pulp fibers and the deposition speed affected the efficiency of orientation. To increase fiber−fiber interaction and produce stronger sheets, partial dissolution of fibers using an ionic liquid can be carried out.[101]

*Electric Field Alignment.* Similar to magnetic field alignment, an electric field can also be used to induce orientation in cellulosic fibers. The fiber orientation will be in the direction of the applied electric field. The electric field orientation of cellulosic fibers was studied by Bordel *et al.*,[102] in which multiscale cellulosic fibers ranging from ramie fragments to CNCs were aligned using electric fields of up to 2000 V/cm. When the cellulosic fibers are at the micrometer scale, Brownian motion will not affect them after the electric field is turned off, but nanoscale fibers might lose their orientation because of the Brownian motion and need to be fixed. The main processing


https://dx.doi.org/10.1021/acsnano.0c07613
ACS Nano 2021, 15, 3646−3673

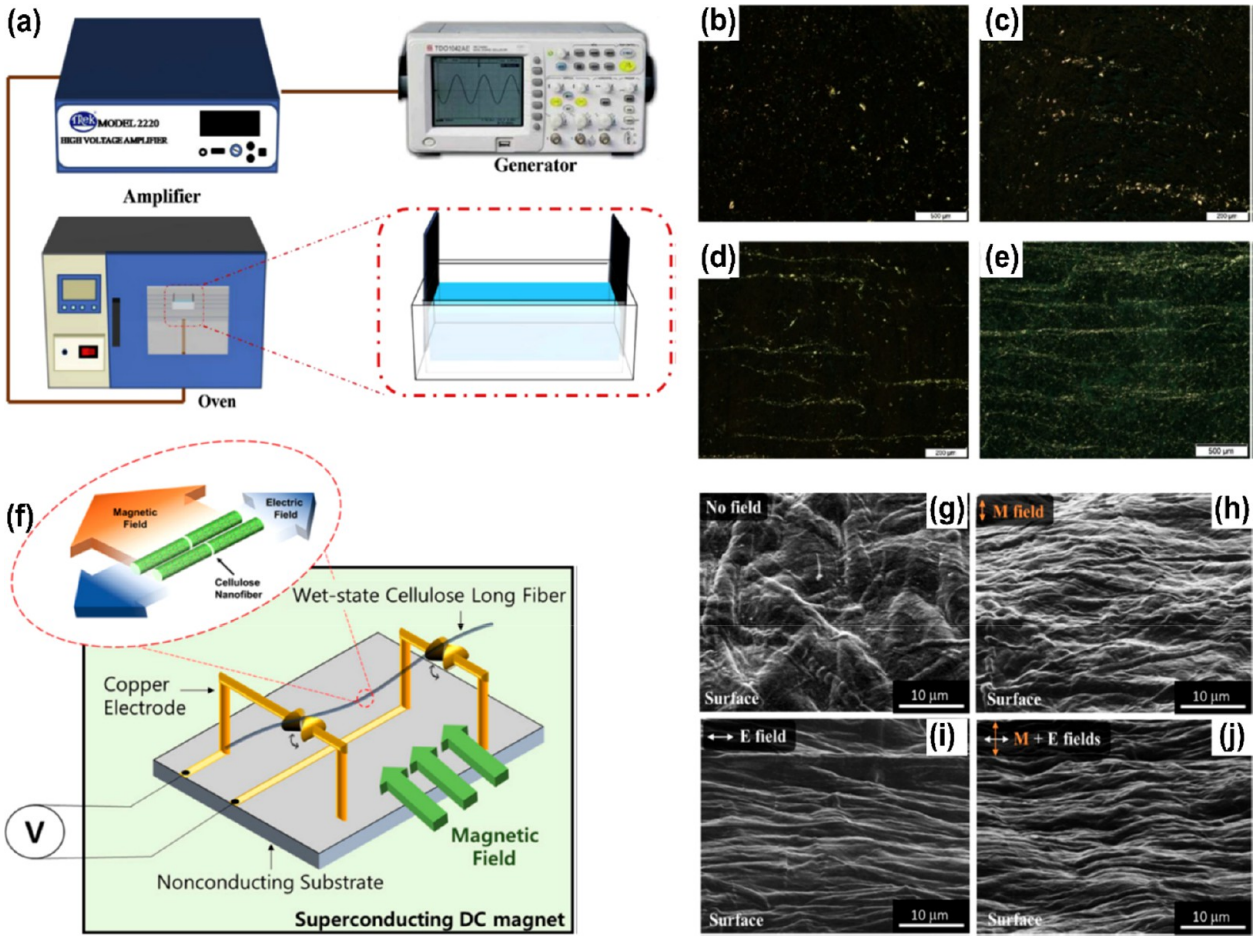


**Figure 2. (a) Experimental setup for fabricating isotropic TPU/TOCNF sample by applying an electric field. POM images of the alignment of TOCNFs in the TPU matrix under (b) 100, (c) 500, (d) 1500, and (d) 2000 V electrical fields at 100 Hz for 30 min. The scale bars in the images are 500 mm. Adapted with permission from ref 86. Copyright 2017 Elsevier. (f) Schematic diagram of the experiment for TOCNFs' alignment by magnetic and electric fields. (g–j) SEM images of cellulose fiber surface with energy field directions. Scale bars in the images are 10 $\mu$m. Adapted with permission from ref 13. Copyright 2019 Springer Nature.**

parameters controlling the electric field alignment of CNFs are electric field magnitude, frequency, and duration of application. Moreover, material properties, including concentration and surface charge, are also important variables influencing the efficiency of electric field alignment.[85]

To maximize the reinforcing efficiency of CNFs in polymers, 2,2,6,6-tetramethylpiperidine-1-oxy radical (TEMPO)-oxidized CNFs (TOCNFs) were aligned under an electric field in a thermoplastic polyurethane (TPU) matrix.[86] A mixture of TOCNFs and TPU in dimethylformamide (DMF) was prepared, and then the mixture was subjected into an AC electric field to induce the alignment (Figure 2a). The degree of alignment of the TOCNFs increased with increasing electric power (Figure 2b–e). Moreover, the subsequent polarization of the fibers was reported, leading to increases up to 2.07 and 1.82 times in tensile strength and elongation at break in the parallel direction of alignment when compared with those in the perpendicular direction.[86] Similarly, an electric field-induced assembly and alignment of silver-coated CNFs in poly(dimethylsiloxane) (PDMS) has been reported.[87] The suspensions were solution-cast between two electrodes, and orientation along the thickness direction was induced using the application of an electric field, leading to improved dielectric permittivity and anisotropic optical properties.

An electrical field can also be used to control the motion of bacteria and further induce the alignment of BC. Sano *et al.* reported a highly oriented BC network produced by *Acetobacter xylinum* by controlling the electric field.[103] By controlling the electrokinetic forces, the authors directed the bacteria while producing BC, to obtain a BC hydrogel with customized 3D morphology with aligned BC. A similar approach was reported to work well for BC production by *Gluconacetobacter xylinus* in the presence of DC electric fields.[104]

*Combination of the Magnetic and Electric Fields.* A combination of magnetic and electric fields can be used to achieve highly oriented cellulose nanofiber materials. When these methods are used together, they can enhance the alignment efficiency. The combined magnetic and electric fields (Figure 2f) were applied to wet-spun TOCNF fibers to improve orientation and mechanical properties.[13] The SEM results (Figure 2g,h) show the improved alignment of TOCNFs under combined magnetic and electric fields compared with others. Although the $f_c$ is only marginally increased from 0.56 to 0.61, when an electric field of 50 V/cm was added to a magnetic field of 5 T, 84 and 125% increments in tensile modulus and strength were observed, respectively.

**Liquid-State Shear and Extensional Methods.** Shear and extensional force-induced alignment is well known in


https://dx.doi.org/10.1021/acsnano.0c07613
ACS Nano 2021, 15, 3646–3673

**Table 1. Comparison of Different Alignment Strategies**

| alignment methods | | cellulose nanofibers[a] | evaluation[b] | $f_c$ ($S$)[c] | outcomes | ref |
|---|---|---|---|---|---|---|
| magnetic field | | CNF | SEM, XRD | N/A | fiber aligned perpendicular to the field in film | 83 |
| | | CNF | POM | | fiber and patterns aligned with chiral nematic domain in film | 84 |
| electric field | | CNF, TOCNF | OM | N/A | fiber aligned along the electric field lines in silicone oil | 85 |
| | | CNF | POM | | aligned in thermoplastic polyurethane, improved tensile strength and elongation at break of nanocomposites | 86 |
| | | CNF[d] | OM, SEM | | fiber aligned in films, enhanced dielectric permittivity and anisotropic light transmission | 87 |
| liquid-state shear and extensional methods | liquid flow | CNF | SAXS, POM | 0.46 | CNF aligned in filament | 88, 89 |
| | | TOCNF | SEM, SAXS, WAXS | 0.92 (0.70) | fiber aligned in filaments, achieved high specific strength and stiffness | 69 |
| | | CNF | SEM, SAXS | (0.39) | | 70 |
| | dynamic and static casting | CNF | SEM | N/A | fibrils partially aligned along the casting direction, higher casting speed results in better alignment | 90 |
| | | TOCNF | POM | | self-aligned into chiral nematic nanopaper with birefringence difference | 91 |
| | | TOCNF | SEM, TEM | | fiber aligned in bulk materials, including hydrogel, aerogel, and film | 92 |
| spinning-induced alignment | dry spinning | CNF | SEM, WAXS | 0.68 | fiber aligned in filament, improved tensile strength and elastic modulus | 61 |
| | wet spinning | TOCNF | SEM, WAXS | 0.72 | | 33 |
| | | BC | SEM, WAXS | 0.69 (0.63) | | 75 |
| | electrospinning | MFC | SEM | N/A | fiber aligned in electrospun composites | 93 |
| | | BC | SEM | | | 94 |
| drawing process | | CNF | XRD | N/A | improved fiber orientation | 95 |
| | | TOCNF | Raman, XRD | | aligned along draw direction, improved tensile strength and elastic modulus | 96 |
| | | TOCNF[e] | POM, SEM, AFM, XRD | | fiber aligned in PLA composites, improved tensile strength and toughness | 46 |
| | | CNF | SEM, WAXS | | fiber aligned in filament, improved tensile strength and elastic modulus | 62[f] |
| templating effects | | TOCNF | micro-CT, SEM | N/A | 3D anisotropic aligned architecture, improved compressive stress and elasticity | 97 |
| | | BC | SEM | | fiber aligned in BC hydrogel | 98 |
| top-down strategy | | CNF | SEM, WAXS | N/A | fiber aligned in macroscopic materials (*e.g.*, film, gel) with high performance | 42, 99 |

[a]MFC, microfibrillated cellulose. [b]XRD, X-ray diffraction; OM, optical microscopy; TEM, transmission electron microscopy; micro-CT, micro-computed tomography. [c]$f_c$, orientation index; $S$, order parameter. [d]Silver-coated CNF. [e]Poly(ethylene glycol)-grafted TOCNF (2,2,6,6-tetramethylpiperidine-1-oxy radical oxidized CNF). [f]Combined with spinning. [g]Combined with hot drawing.

many material systems, as these forces are inherent in many processes, such as extrusion, tape casting, or fiber spinning. The paper-making process, such as the Fourdrinier machine, is a common commercial example of this alignment method.[105] High aspect ratio particles such as CNFs can orient parallel to the flow direction in shear or extension, so some level of preferential alignment or degree of orientation is often expected. Processes are often intentionally designed to optimize the conditions that produce alignment to achieve beneficial effects on materials properties, such as anisotropy. Achieving flow-induced alignment in CNF and CNF-composite materials depends on various factors, including the particle length, type, and concentration, which are important in determining the solution's viscosity. Because of the high entanglement density of CNFs, broad length distribution, and particle−particle interactions, CNF solutions exhibit higher viscosity than their rod-like CNC counterparts. Although many studies have demonstrated alignment in CNC materials, CNF alignment is a more complex process and thus a comparatively less researched topic. The next section discusses various alignment strategies in which shear and extensional forces are the primary means of obtaining CNF alignment in neat and composite CNF materials. These strategies include liquid flow, dynamic and static casting (roll-to-roll, tape casting, evaporation), and extrusion methods.

*Liquid Flow.* Liquid flow is a precursor in many processes, and understanding how orientation occurs through a channel could be beneficial in creating aligned CNF structures. For instance, there are several examples of shear stresses inside a die facilitating alignment before solidification in wet-spun CNF fibers (as evidenced by the orientation of as-spun fibers). Additionally, extensional forces capable of elongating and aligning CNFs occur during flow-assisted strategies for fiber formation.[13,75,88,89,106] Because alignment occurs through


https://dx.doi.org/10.1021/acsnano.0c07613
ACS Nano 2021, 15, 3646−3673

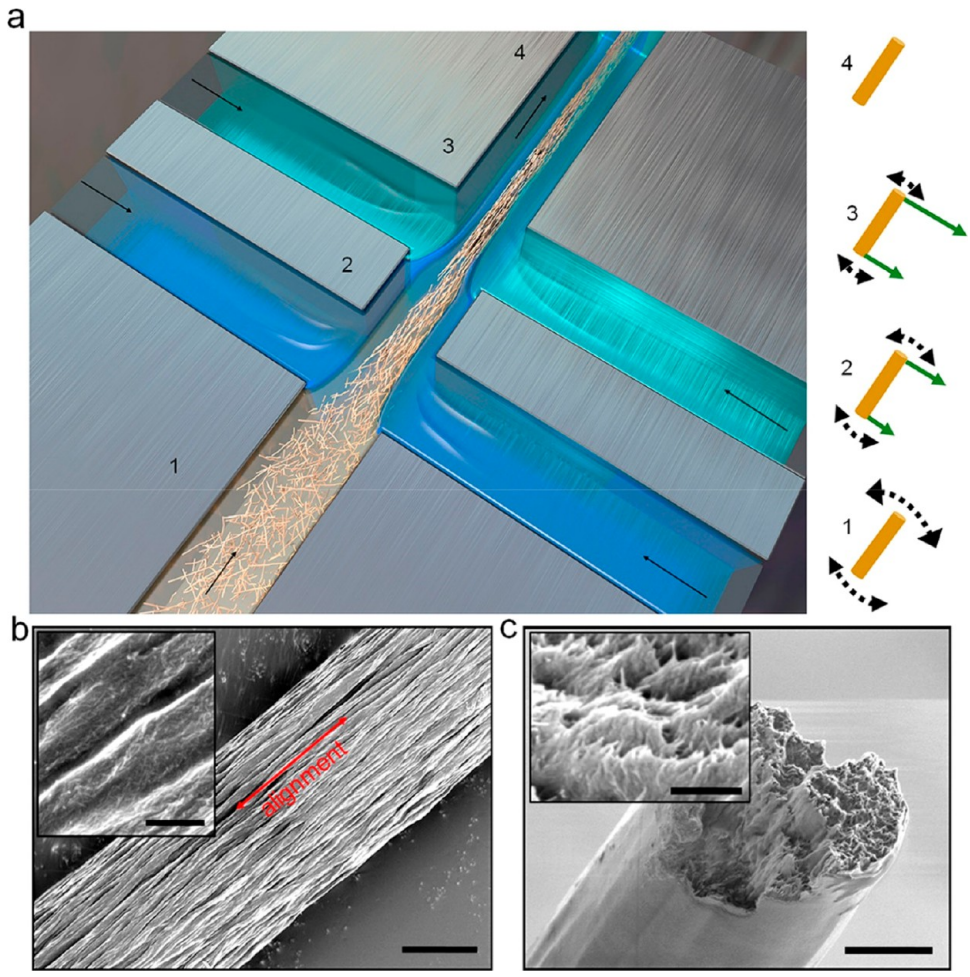


**Figure 3. Flow-assisted formation of CNF fiber reproduced from Mittal *et al.*[69] (a) Schematic of channel and nanofiber path (rotational and translational motion of nanofibers shown adjacent). SEM images of (b) alignment along fiber direction and (c) fiber cross-section. Scale bars in (b) and (c) are 3 $\mu$m, and insets are 400 nm. Reproduced with permission from ref 69. Copyright 2018 American Chemical Society.**

rotation and translation of nanoparticles in solution, CNF orientation in different flow configurations has been studied by several researchers.[70,89,107,108] Rosen *et al.* studied the orientation of CNFs (and CNCs) in dilute and semi-dilute concentrations under confined flow. At low flow rates, semi-dilute CNFs were relatively aligned, but at higher flow rates, alignment appeared to become independent of flow rate. For CNFs, the lack of dependence on flow rate at high flow rates could be due to self-entanglement or fibrillar entanglement, which can cause bundles to rotate with local vorticity rather than elongating and orienting in the direction of flow. CNFs are flexible, long nanoparticles which feature a large disordered region that imparts deformation-induced bending or folding at high shear rates due to the presence of physical kinks and fiber dislocations. Moreover, under shear, particles perpendicular to the direction of shear will rapidly orient parallel to the direction of flow but can tumble or flip faster than in pure extensional flow, resulting in earlier loss of alignment.[89] Likewise, modifying CNFs' length can result in more easily aligned nanoparticles but can also lead to more rapid relaxation and disorganization due to the higher diffusivity of smaller nanoparticles.[69] Electrostatic fibril interactions did not appear to significantly affect the rotational diffusion process.[89]

Alignment in flow-assisted methods depends on the relationship between the time scales for alignment, diffusion, and solidification.[69,70] Modifying parameters that change one or more of these time scales (*e.g.*, ion exchange or particle length) will likely affect the overall orientation.[70,89] The work by Mittal *et al.* is extremely informative on the importance of balancing Brownian motion, intermolecular forces like electrostatic repulsive forces,[69] and mechanical entanglement to achieve highly oriented CNFs. In the flow-focusing method developed by Mittal *et al.* (Figure 3), a TOCNF slurry in a channel was subjected to two crossflows: first, deionized water to direct the nanoparticle stream, and second, an acidic solution to trigger protonation of surface carboxyl groups and begin fiber consolidation by reducing electrostatic repulsion of the nanofibers. Shear flow helps initially align the CNFs when the core flow enters the channel at 4.1 mL/h, but extensional flow is dominant once the CNF stream is subjected to the first and secondary crossflows, 4.4 mL/h and 24.6 m/h. The net effect is a higher packing order, low porosity, and high alignment of TOCNFs, attributed mostly to extensional forces present in flow-focusing channels like the one employed.[69,89] Between the CNFs tested, CNFs with larger lengths (590 nm) exhibited slightly higher local ordering on average during processing compared to the smallest (391 nm long) due to the longer rotary diffusion times of larger particles. Consequently, CNF macrofibers composed of larger CNFs (590 or 683 nm long) exhibited higher order parameters (0.7 for CNFs 590 nm


https://dx.doi.org/10.1021/acsnano.0c07613
*ACS Nano* 2021, 15, 3646−3673

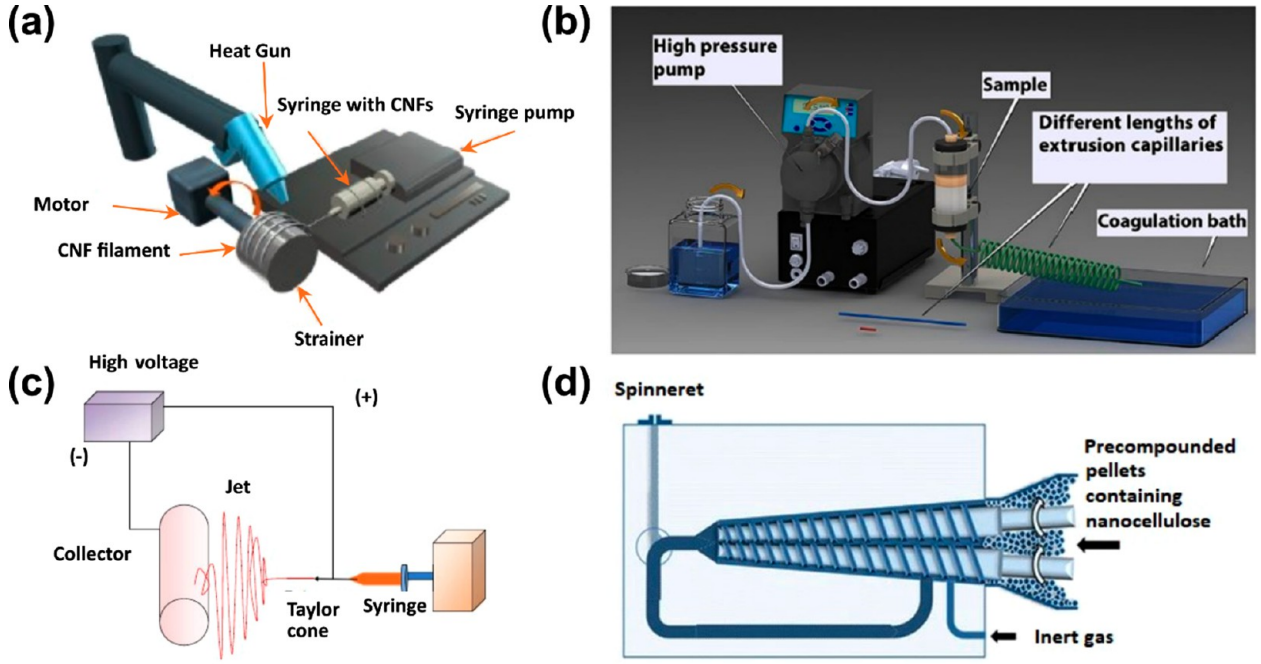


**Figure 4. Schemes of different fiber spinning processes: (a) Dry spinning. Reproduced from ref 119 under terms of the CC-BY license. Copyright 2017 MDPI. (b) Wet spinning. Reproduced from ref 74 under terms of the CC-BY license. Copyright 2017 Springer Nature. (c) Electrospinning. Adapted with permission from ref 122. Copyright 2015 Institute of Food Technologists. (d) Melt spinning. Reproduced with permission from ref 123. Copyright 2014 Springer Nature.**

long), which translated to greater strength (~1200 MPa) and stiffness (50−70 GPa), while the shorter CNFs (391 nm) exhibited a low order parameter (0.53) and comparatively low mechanical strength (630 MPa) and stiffness (45 GPa).[69]

Orientation can also be induced during the synthesis of nanoparticles.[109,110] Luo *et al.* reported a method to induce alignment of BC for application in tissue engineering.[109] They used a fermenter equipped with a rotating blade which forces the bacteria to move along the outside of the cylinder in one direction; consequently, the BC grew along the path of rotation, where the velocity at the wall was 30, 90, or 150 mm/s. While the highest alignments were obtained by increasing the velocity at the wall, the production rate and crystallinity index of the BC decreased. The maximum production rate decreased from ~55 to 25 mg/mL (55% change), and the crystallinity dropped from 91% to 77% for the fastest velocity. Krystynowicz *et al.* observed a similar effect on the production rate in their investigation of velocity on BC cultivation.[111]

*Dynamic and Static Casting.* Shear stresses can be high enough in solvent-casting methods to generate some preferential alignment. Pahimanolis *et al.* developed a tape-casting method to create carboxymethyl cellulose (CMC) and non-oxidized CNF nanocomposite films and explored the effects of casting speed (0.3 and 1.9 m/s) and CMC content (up to 30 wt%) on CNFs' alignment.[90] At the highest casting speed, the authors observed that CNF/CMC tape alignment increased because of the higher shear stress created at the interface, with this effect being most pronounced for the highest CMC concentration; the CMC is thought to have a lubricating effect on CNF bundles.[90] In CNC/poly(vinyl alcohol) films produced roll-to-roll, the opposite was shown, suggesting that a critical concentration (above 50%) of the smaller aspect ratio CNCs was needed to obtain alignment in coatings.[112] If and at what aspect ratio this transition in behavior occurs for CNFs is an area for future study, as CNFs can exhibit a wide range of aspect ratios and considerable size polydispersity. However, the overall order obtained by tape casting ($f_c$ of 0.05 maximum) was comparatively low compared to those obtained with other processes, potentially due to relaxation of the film during the drying process or insufficient shear force.[90] Roll-to-roll processing of CNFs has been investigated as well.[113] In addition to CNF content (1 or 2 wt% CNFs depending on the feeding pressure of the die), CMC was investigated as an additive, but in small amounts (10 pph maximum), which as used to reduce the viscosity of the CNF solution. However, high production rates, where shear rate on the material would also be high, were not possible due to the high water content of solutions, and instead the production rates obtained (0.02−0.5 m/s) were comparable to those obtained with the tape-casting method. While the slot gap die (500−1000 $\mu$m) was varied to meter coating thickness, it limited the maximum coating speed for the material, as the coating had to dry. While roll-to-roll processing has been successfully demonstrated to induce alignment along the rolling direction in CNC coatings, orientation in CNF coatings produced by this method has not been studied explicitly.[114] Balancing water content and composition to obtain low-viscosity solutions for processing, but that do not inhibit higher production rates that would result in larger shear forces on the material, is still a challenge for CNFs and a barrier to developing scalable technologies for these materials.

Although casting methods such as roll-to-roll and tape casting hold practical significance as scalable processes, the static casting of CNF solutions followed by evaporation has provided some valuable insights into the governing parameters for facilitating self-induced alignment in CNFs. Uetani *et al.* studied the formation of "coffee-rings" in evaporated droplets and spray-dried morphologies for rod-like tunicate CNCs and CNFs having very similar zeta potential values.[115] Although evidence was qualitative, SEM images of the CNCs exhibited


https://dx.doi.org/10.1021/acsnano.0c07613
ACS Nano 2021, 15, 3646−3673

an ordered outer ring, with CNCs running parallel to each other and the outside band. Conversely, the CNF coffee ring did not exhibit strong evidence of self-organizing behavior. As mentioned earlier, this may be attributable to the longer diffusion times of long CNF particles. Other studies have shown that evaporation/condensation of CNFs can exhibit self-organizing behavior.[91,92] Uetani *et al.* observed self-organization of a chiral nematic phase during evaporation and identified the concentration at which the onset of self-organization began at the surface where evaporation was occurring.[91]

**Spinning-Induced Alignment.** Fiber spinning comprises an array of fiber formation processes that produce continuous filaments.[116] Because of the commercial importance of fiber spinning technologies in macroscopic filament production, spinning-induced alignment of CNFs will be discussed in detail. Spinning methods typically include solvent spinning and melt spinning (Figure 4), where solvent spinning can be categorized into dry spinning, wet spinning, and electrospinning.[117] As a common starting material, polymers are melted or dissolved in solvents to form spin dopes. These spin dopes are then forced through a needle, die, or spinneret to form a continuous string. The solidification mechanism depends on the processes: for melt spinning, solidification occurs during cooling; in dry spinning, it occurs through solvent evaporation; and in wet spinning, it occurs by precipitation of the filament in an antisolvent.[117] The extrusion involved in spinning provides early-stage alignment of the fibers.[63] Further alignment stems from the filament stretching, where a rate difference exists between the collector speed and the fiber spinning speed, or simply by a post-process cold drawing.[62,118] Factors influencing the properties of spun CNM filaments cover both material-related parameters (additives, CNM source, pretreatment method, solid volume fraction, crowding factor, and rheology) and spinning-related parameters (shear rate, drawing ratio, coagulation, and drying).[117] Spun fibers are widely used as filters, textiles, and composites.[15] Extensive research has proven that spinning processes are efficient ways of producing CNM filaments with high mechanical performance and multiple functionalities.[117]

*Solvent Spinning. (1) Dry spinning.* The process of dry spinning is illustrated in Figure 4a, where the CNF suspension is loaded into a syringe and pumped out through a needle, where a heat gun evaporates the solvent and the filament is collected on a substrate.[15] The alignment of CNMs is induced primarily when they are forced to pass through the narrow channel inside the needle but also from rotation of the collector. Several studies have examined applying dry spinning to successfully obtain CNF filaments from their suspensions.[61,62,118−120] Dry spinning has also been performed on CNM/polymer composite dopes.[121]

*(2) Wet spinning.* Compared with dry spinning, the dope in wet spinning enters an antisolvent or coagulation bath after exiting the formation element. Here, the fibers precipitate from their dope solvents because of the solvent-exchange process, as shown in Figure 4b.[116] The antisolvent or coagulation bath is a medium that exchanges the dope solvent for rapid dehydration. The depletion of solvent brings fibers in contact, inducing extra alignment to the fibers.[73] In general, a rotary collector is connected to collect the fiber from the bath and can further induce the fiber alignment during the fiber collection. In dry spinning of CNFs, removing the dope solvent requires a fair amount of energy and time, especially with aqueous suspensions in which a large amount of water exists. Therefore, wet spinning provides an efficient option for tackling the drying issue of CNMs.[116]

*(3) Electrospinning.* Electrospinning requires an electrostatic field between a needle tip and a collection substrate, as shown in Figure 4c.[122] Electrospinning begins with a conductive dope forming a tiny Taylor cone at the tip of a needle.[124] The cone spins into multiple jets, the diameters of which are reduced to sub-micrometers under a proper electrostatic force. Because the jets are sufficiently narrow and possess a high surface area, the dope solvent evaporates rapidly.[94] A separate set of material and processing-related factors influence the final fiber characteristics, including collector type, tip-to-collector distance, voltage, injection rate, CNM type, dope conductivity, surface tension, humidity, and so on.[116] Fibers are typically aligned inside a spun yarn, attributed to a combination of the dielectrophoretic force and shear force during electrospinning.[125] The structure of the electrospun yarns is normally not aligned; instead, they exist in the form of a non-woven mat. To further align the yarn, various approaches are applied at the collection end,[125] such as increasing the collector rotation speed and using a collector comprised of two conductive substrates separated by a void gap.[125−128] Electrospinning of CNFs is often performed on CNF−polymer composites from a polymer solution with CNFs as an additive.[116,129] To our best knowledge, studies on electrospinning of neat CNFs are not reported in the literature. However, electrospinning itself could produce cellulose nanofiber from cellulose solutions,[130,131] especially in solvents such as dimethylacetamide/lithium chloride (DMAc/LiCl),[132] ionic liquids,[133] and alkali/urea, where cellulose has solubility.[134]

*Melt Spinning.* Melt spinning processes materials in their molten state and is used extensively for thermoplastic polymers with sufficient spinnability, as shown in Figure 4d. Melt spinning of pure CNMs is difficult because the melting temperature (260−270 °C) of cellulose is close to its decomposition temperature (260−270 °C). Instead, melt spinning can be performed on CNFs-reinforced thermoplastic composites.[80,123,135−137] However, few studies have reported on the alignment of CNFs in a polymer by melt-spinning processes. Such a low research interest relates to an already-existing issue of a broader research topic, *i.e.*, the agglomeration of CNMs in polymers during melt processing.[136]

**Drawing Processes.** Drawing processes (also called "mechanical stretching" in the literature) rely on the application of mechanical force to align and elongate (straighten out) nanoparticles, which is desirable to maximize the property improvements of these anisotropic materials. For cellulose nanofibers, these processes have been primarily uniaxial stretching to date. However, a variety of drawing conditions, including variations in temperature, humidity, water content, strain rate, and load, have been explored for cellulose nanofiber and its composites. Here we will differentiate between cold-drawing and wet-drawing processes. Cold-drawing processes are understood to be processes performed at an elevated temperature in a dry environment, but below the melting point of the materials being drawn; wet-drawing processes will be defined as any process in which the materials are subjected to humidity, soaked, or submerged in a solvent (typically water) to enhance drawability.

*Cold Drawing.* Cold drawing of CNF composites has shown improvement over a broad range of concentra-


https://dx.doi.org/10.1021/acsnano.0c07613
ACS Nano 2021, 15, 3646−3673

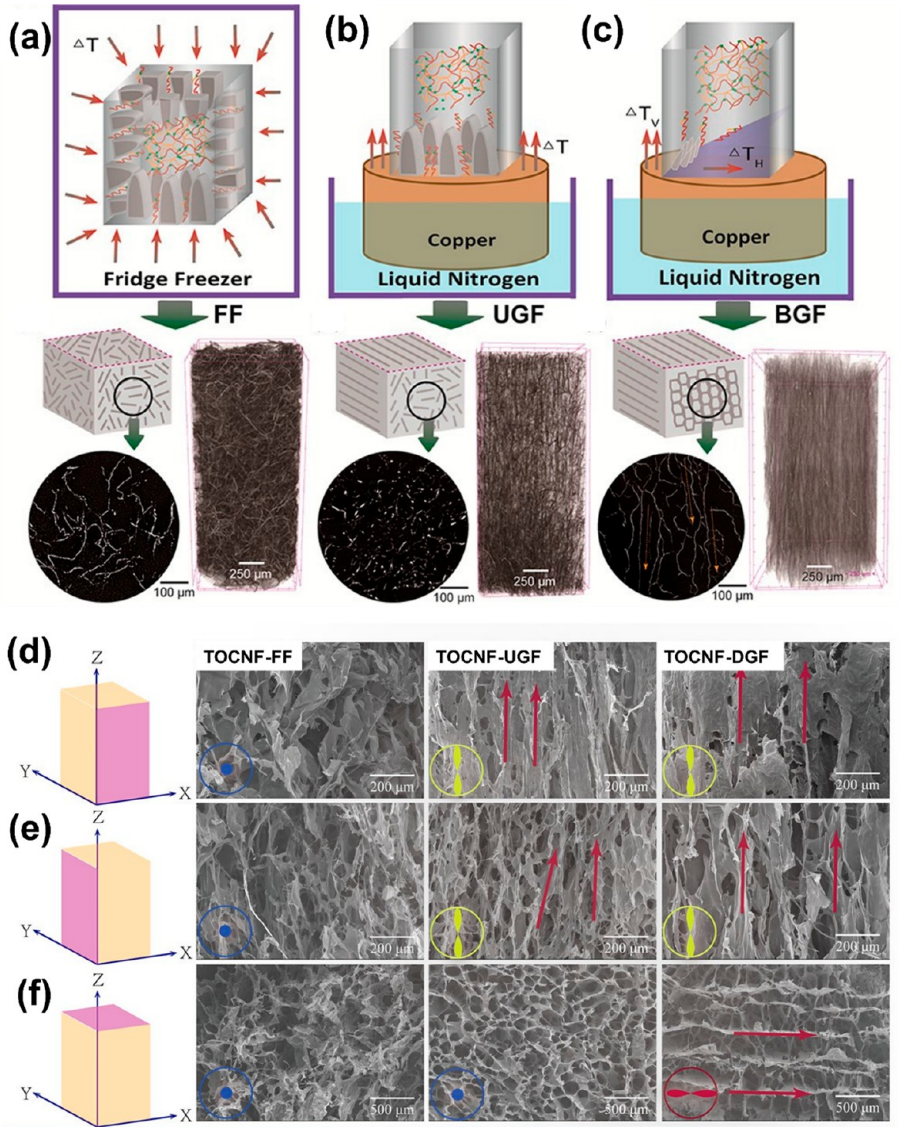


**Figure 5. Scheme of ice templating and micro-CT scanning 3D morphology of nanocellulose foams manufactured by (a) bulk freezer freezing (FF), (b) unidirectional gradient freezing (UGF), and (c) bidirectional gradient freezing (BGF). (d–f) SEM images of three different directions (XZ, YZ, and XY) of TOCNF foams from TOCNF-FF, TOCNF-UGF, and TOCNF-BGF techniques. Adapted with permission ref 97. Copyright 2019 American Chemical Society.**

tions.[46,62,80,138,139] Cold-drawn plasticized polylactic acid (PLA)/CNF composites prepared by Geng *et al.* exhibited high toughness and ultimate tensile strength compared with similar materials with only 0.1 wt% TOCNFs or modified TOCNFs.[46] Likewise, Clarkson *et al.* demonstrated that melt-spun PLA/modified CNF composite (mCNF) fibers with concentrations up to 1.25 wt% mCNFs exhibited improved stiffness with cold drawing, but the alignment of PLA along the tensile axis decreased with increasing CNF content, despite the overall improvement in polymer order with cold drawing.[80] However, because of the low concentrations of CNFs used in both studies, the alignment of CNFs could not be confirmed in either case. These studies were performed at elevated temperature and low concentrations, so high draw ratios could be obtained. For materials where CNF is the matrix, like those of the dry-spun filaments of hydroxyethyl cellulose (HEC)/CNF and pure CNFs studied by Hooshmand *et al.*,[62] cold-drawing becomes very challenging. To cold-draw nanocomposite fibers, Hooshmand *et al.* implemented a series of fast and slow displacement rates, followed by a relaxation step to prevent premature failure during drawing. The HEC/CNF nanocomposites exhibited a higher orientation index in both the as-spun and drawn samples compared with neat CNF fibers produced by the same methods. In addition to acting as a wet strength additive during fiber spinning, HEC improved the ductility of the fibers, which allowed them to be drawn to a slightly higher drawing ratio compared with the neat CNFs.

*Wet Drawing.* Wet drawing of CNF films uses residual water from the production process or a humid environment to facilitate drawing.[75,96,140,141] Residual water in the partially dry CNF material acts as a plasticizer by disrupting hydrogen bonding between neighboring particles. However, wet drawing depends on factors such as the drying conditions, water content, and relative humidity of the drawing environment. Baez *et al.* evaluated the effect of different drying conditions on the structural and physical property development in TOCNF films: fully and partially restrained, and uniaxially drawn.[96] The wet-drawing process enabled films to be drawn up to 40% of


https://dx.doi.org/10.1021/acsnano.0c07613
*ACS Nano* 2021, 15, 3646–3673

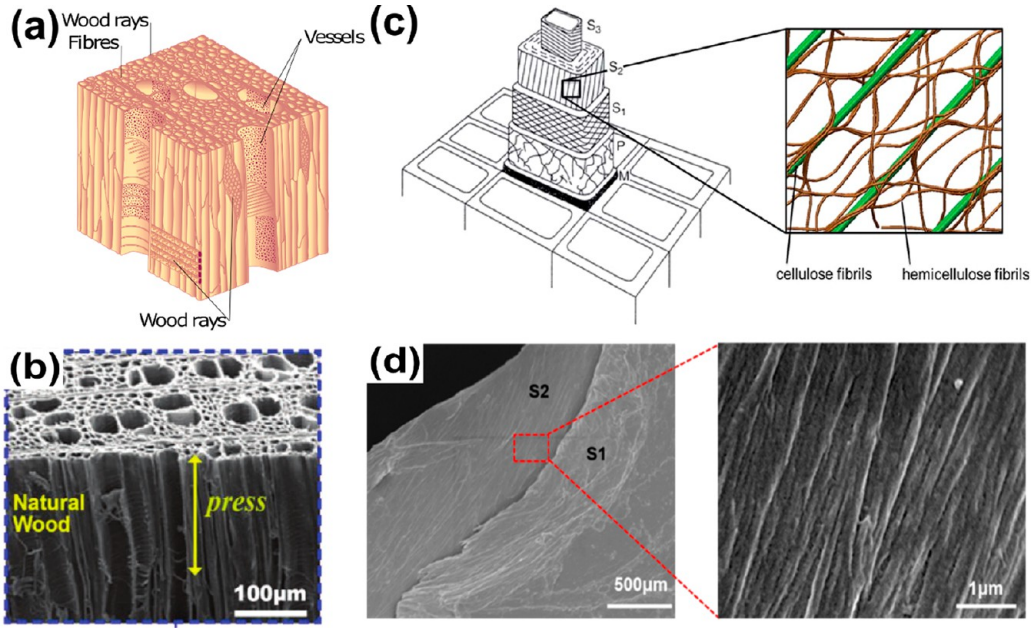


**Figure 6. (a) Schematic depiction of the wood microstructure. Adapted with permission from ref 178. Copyright 2020 Springer Nature. (b) SEM image of natural wood, showing the microstructure of wood. Adapted with permission from ref 99. Copyright 2019 Wiley-VCH. (c) Schematic of cell wall layers within cellular structure. Adapted with permission from ref 168. Copyright 2013 Royal Society of Chemistry. (d) Cellulose nanofibrils' orientation in the S2 layer of the fiber cell wall. Adapted with permission from ref 169. Copyright 2020 Elsevier.**

the original length, and uniaxial alignment along the tensile direction increased with increasing drawing ratio. Drying the aligned material under tension is common in wet-drawing processes to control/limit shrinkage and loss of orientation due to relaxation. Similarly, tension is used in the oxidation process of polyacrylonitrile fibers to create carbon fibers or during solidification during fiber processing.[142−145] Films and membranes made by vacuum filtration of CNFs normally undergo in-plane shrinkage upon drying if not restricted. If such wet films are cut into ribbons and fixed at both ends, the drying-induced shrinkage will also induce reorientation of CNF fibrils along the length of the ribbon.[81]

Several examples of wet-drawing to enhance CNFs' alignment and consolidation have been investigated for CNF filaments as well. Wet-spun TOCNF filaments were wet-drawn in water using a stretching device capable of applying strain-rate-controlled deformations.[78] TOCNFs were also aligned by mechanical wet stretching up to 50% by Josefsson *et al.*[95] The highest mechanical properties (Young's modulus of 37.5 GPa and tensile strength of 543.1 MPa) were reported by Kim *et al.* when wet-spun CNFs were wet stretched up to 20%.[146] Finally, by covalent grafting of PEG onto TOCNFs, high orientation and consequently high mechanical properties were achieved.[147] In another study, by Wang *et al.*, BC macrofibers were prepared by cutting the BC pellicle into rectangular strips, mechanically drawing the wet pellicle, twisting to form a cylinder, and setting the shape by drying under tension.[140] Orientation has generally improved mechanical performance, porosity, and defects in CNFs and CNF-based materials. Yao *et al.* prepared macrofibers of aligned BC using a wet-spinning and wet-drawing method, followed by cross-linking the fibers with multivalent ions.[75] Similar to previous studies, undrawn, as-spun fibers produced with higher extrusion rates yielded fibers with a higher relative degree of alignment. Although increasing the concentration for a fixed extrusion speed did not further enhance alignment, fibers prepared from higher concentrations exhibited superior mechanical properties, perhaps because of better fiber consolidation (higher density, less porosity).

**Aligning Cellulose Nanofibers through Templating Effects.** Templating techniques have been used extensively to achieve ordered structures, including aligned particles within a material. When it comes to using templating strategies to align cellulose nanofibers, one main approach in the literature is ice templating. This technique uses growing ice crystals within a liquid medium and relies on the principle that ice crystals only grow within the solvent, expelling any solutes present.[15,148−152] For cellulose nanofiber templating and alignment, the ice crystals grow, expelling the cellulose nanofiber and shearing it between adjacent ice crystals. These shear forces, between both the cellulose nanofiber and ice crystals and adjacent cellulose nanofibers, serve to align the fibers. The frozen ordered structure is then sublimed, usually using a freeze-dryer, to produce aligned cellulose nanofibers.

There are three approaches for ice-templating (Figure 5a−c): bulk freezer freezing (FF), unidirectional gradient freezing (UGF), and bidirectional gradient freezing (BGF).[32,151−155] Chen *et al.* compared these three methods of ice templating and determined that temperature-gradient-directed methods produce repeatable aligned structures.[97,156] One of the easiest and most common methods utilized is UGF (Figure 5b).[157] A temperature gradient is applied in one direction, and ice crystals grow slowly parallel to the freezing direction, forming channels between crystals. In systems with very low CNF concentration, CNFs are aligned between ice crystals in an isotropic fibril structure. When the concentration of CNFs is increased, the ice crystals result in alignment of anisotropic CNF structures.[154] All these aerogels display a honeycomb-like porous structure, aligned along the XZ and YZ directions, relative to the original direction of ice growth (parallel to the *z*-axis). Along the XY direction, the material is isotropic, featuring erratically shaped pores (Figure 5d−f, TOCNF-


https://dx.doi.org/10.1021/acsnano.0c07613
*ACS Nano* 2021, 15, 3646−3673

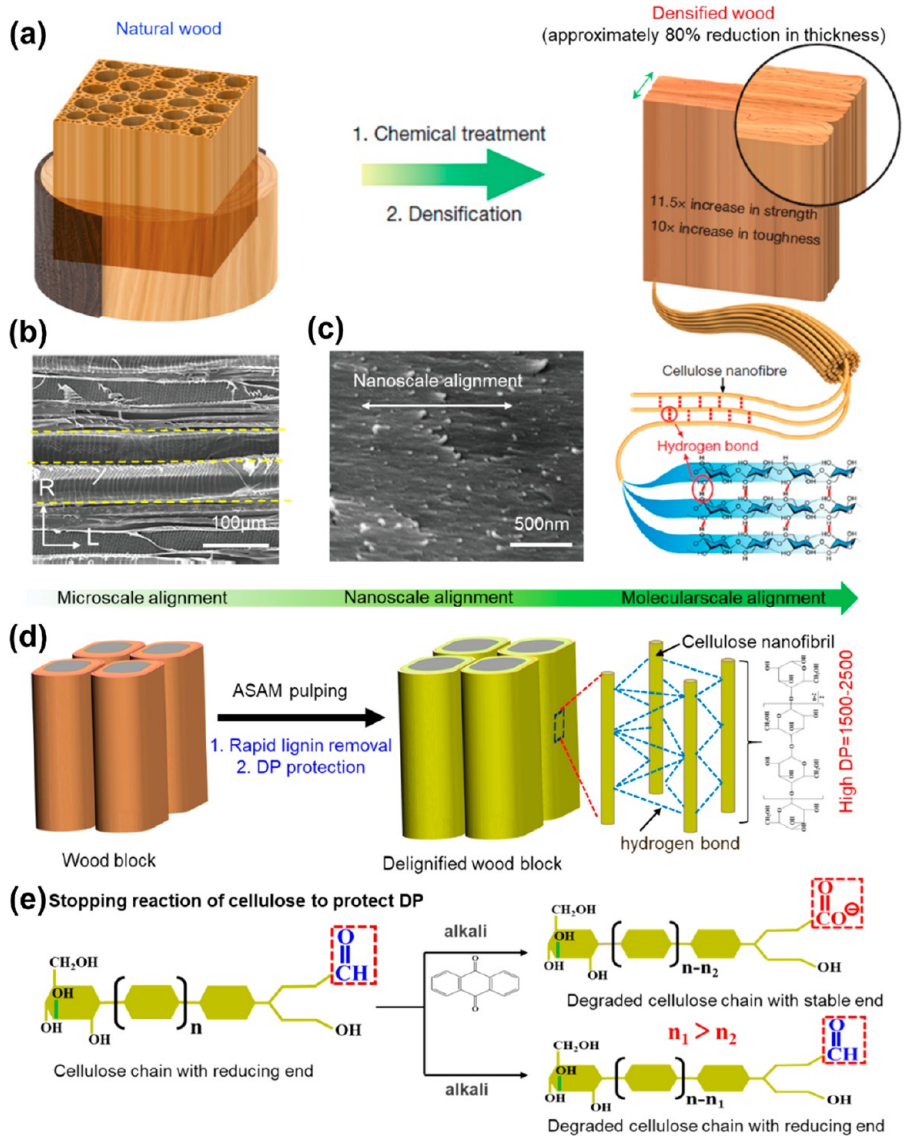


**Figure 7. (a) Schematic of the top-down two-step approach to transform bulk natural wood directly into superstrong and tough densified wood. (b) SEM image of the natural wood sample, showing the highly aligned cellulose cell walls. (c) SEM image of the densified wood, showing the highly aligned cellulose nanofibers. Adapted with permission from ref 42. Copyright 2018 Springer Nature. (d) Schematic illustration of the ASAM pulping of wood blocks that degrades the lignin rapidly while achieving a high DP of cellulose. (e) The stopping reaction between reducing end units in the cellulose chains and anthraquinone under alkaline condition. Adapted with permission from ref 169. Copyright 2020 Elsevier.**

UGF). Alternatively, methods involving bidirectional or multidirectional temperature gradients are being developed (Figure 5c). The presence of a multitude of freezing directions results in complex ice structures, with the templated CNFs aligning into intricate shapes. These aerogels feature CNFs aligned along all three axes, relative to the original directions of ice growth (both parallel and perpendicular to the *z*-axis): XY, XZ, and YZ (Figure 5d–f, TOCNF-BGF). The final structure is completely anisotropic and features a combination of sheets and channels. Bulk ice templating can be used, but the resultant materials are non-aligned aerogels (Figure 6a). Because of a lack of directional ice growth, no axis-oriented alignment is observed in these materials (Figure 5d–f, TOCNF-FF).

Templated materials can also be used to align cellulose nanofibers. One main technique is to synthesize aligned BC, where BC epitaxial growth occurs along a template.[98,158−160] In this approach, a template material is used to assign boundaries for the growing bacterial chain. By using a template, BC can be grown in a specific fibril alignment, providing higher mechanical performance and better suitability for medical usage. These template materials can be polymers, synthetic choices (such as PDMS), natural polymers (including aligned cellulose materials), or inorganic materials (such as silicates). These templates always have pre-defined channels or patterns for BC growth. Putra *et al.* used a series of silicone tubes to grow BC with specific dimensions.[98] Thicker wall dimensions allowed the BC to grow along the curved surface and provided stable tubular BC even after removal of water. Growth of the BC was repeatable and displayed minimal irregularities. Similarly, Putra *et al.* also used ridged PDMS surfaces to grow BC.[158] The PDMS mold displays good oxygen permeability, which allows for optimal growth of the


https://dx.doi.org/10.1021/acsnano.0c07613
*ACS Nano* 2021, 15, 3646−3673

BC. This template resulted in uniaxially oriented, anisotropic BC with superior mechanical properties.

The use of natural polymers as a template for BC growth typically requires synthesis of the template materials first. For cellulose specifically, most of the research revolves around the use of templated nematic ordered cellulose (NOC) systems, as termed by Kondo *et al.*[161] This approach uses DMAc/LiCl to selectively swell cellulose fibers, causing realignment of the hydroxyl (OH) groups on the glucose rings.[162] This solution is then slowly drawn, causing a gelation between the aligned cellulose chains and penetrating water molecules, which further results in a highly aligned, nanocrystalline cellulose with available OH groups. The availability of these OH groups is key to utilize these NOC materials as templates for BC growth.[159] To maintain alignment of the growing BC, OH groups located on carbon 6 need to be able to anchor and adhere the growing fibers in place on the NOC matrix. Kondo *et al.*'s results also suggested the addition of chitin, and in the NOC supports have an amplitude change in the growing BC due to an alternation in position of the C6 hydroxyl group on the chitin template.[163,164] The final wiggled BC maintains this shape and shows great promise for further development of autonomous nanofabrication of BC.

## TOP-DOWN STRATEGY TO ALIGN CELLULOSE NANOFIBERS

Although CNFs can be aligned by various bottom-up assembly strategies as described in the previous section, these strategies can be production-intensive.[33,63,70,78,85,139,147,154] Additionally, realizing anisotropic hierarchical structures across different length scales in the same material is difficult. Contrary to bottom-up fabrication, top-down fabrication takes advantage of the existing hierarchical structure in an object to manufacture multifunctional materials by removing the extraneous components inside. Wood has an anisotropic structure with pronounced alignment of constituent cellulose fibers at different sizes.[1,2,5,165,166] At the microscale, the cellulose fibers and the lumina of the vessels are largely aligned along the growth direction of the tree (Figure 6a,b).[99,167] On the nanoscale, CNFs in the cell wall, especially in the S2 layer, are oriented almost parallel to the cell axis (Figure 6c,d).[168,169] Additionally, at the molecular scale, the crystalline cellulose chains are strictly aligned. The orientation of cellulose fibers at different hierarchical levels in natural wood makes it possible to achieve the alignment of CNFs by simple top-down strategies. For example, in the wood industry, many top-down strategies combining pre-treatment (heat, steam or cold rolling) and densification have been applied to enhance the mechanical properties of natural wood by utilizing its near-perfect orthotropic hierarchical structure.[170−177] However, the existing strategies currently face difficulties in achieving complete densification and stable dimension of the densified wood, thus resulting in expansion and weakening in humid environments.[177] Therefore, interest in achieving alignment of CNFs using top-down fabrications by directly taking advantage of the anisotropic hierarchical structure of natural wood has not waned, because of its simple and efficient methodology compared with traditional bottom-up alignment strategies.

The latest developments in top-down strategies for achieving alignment of CNFs have been demonstrated by Hu *et al.* and involve the partial removal of lignin/hemicellulose from natural wood, followed by hot pressing (Figure 7a).[42] Partial removal of lignin and hemicellulose (using $NaOH/Na_2SO_3$) from the cell walls decreases the rigidity of the delignified wood, which facilitates densification of delignified wood by mechanical pressing. During densification, wood lumina and the porous wood cell walls collapse entirely, facilitating inherent alignment of CNFs in the cell wall of wood directly, leading to a much more densely packed structure (Figure 7b,c). Therefore, this modified wood with densified features and aligned CNFs exhibits much higher strength (587 MPa) than natural wood (51.6 MPa) and higher specific strengths ($422.2 \pm 36.3$ MPa cm$^3$ g$^{-1}$) than almost all structural metals and alloys.[42] Similarly, combining the complete delignification with mechanical compression can easily align CNFs in transparent films and "cooling wood".[25,82,179−181] Zhu *et al.* reported an anisotropic transparent film with aligned CNFs, obtained by pressing completely delignified wood to remove the porous structure entirely,[25] which is a much more effective and scalable strategy than that of manufacturing transparent paper from CNF. The transparent film not only exhibits excellent optical properties (over 90% light transmittance and high haze) but also exhibits a good mechanical strength (up to 350 MPa), attributable to its densified and anisotropic structure.[25] However, the strength of the transparent film and "superwood" is still far inferior to the strength of individual wood CNFs, which mainly results from the degradation of cellulose during delignification.[37] Additionally, aligned CNFs made by top-down strategies have also been obtained using complete delignification of wood, which produces an orientation structure and gives the materials desired functions.[182−185] For example, white wood (also called "nanowood") with hierarchical alignment of CNFs can be fabricated by a scalable top-down approach *via* simple chemical delignification (using combined $NaOH/Na_2SO_3$ and $H_2O_2$).[185] The nanowood has a low thermal conductivity (0.03 W/m·K) in the transverse direction because of its aligned structure. Interestingly, the anisotropic structure of the nanowood results in its anisotropic thermal conduction properties.

In top-down CNF aligning strategies, directly inheriting the anisotropic structure from wood is paramount and delignification plays a critical role. Unfortunately, during delignification, the high temperature, alkaline conditions, and presence of oxidizing bleaching chemicals cause degradation of cellulose, thus resulting in deterioration of the intrinsic properties of CNFs, which further affects the properties (such as mechanical and thermal properties) of the ultimate cellulose materials. Therefore, cellulose should be protected from degradation during delignification. Most recently, Fang *et al.* demonstrated a top-down method combing alkaline sulfite−anthraquinone−methanol (ASAM) pulping and mechanical pressing to produce strong anisotropic nanocellulose films by a cellulose degree of polymerization (DP) protection strategy (Figure 7d).[169] ASAM pulping can remove the lignin and hemicellulose from natural wood quickly while maintaining a high DP of cellulose resulting from the synergistic effect of rapid lignin removal and prevention of the peeling reactions between cellulose chains (Figure 7e). As-prepared nanocellulose film exhibited a superb tensile strength of up to 1.13 GPa and specific tensile strength (820 MPa cm$^3$ g$^{-1}$) much higher than those of current natural polymers. In addition to the DP of cellulose, the wood species, the density of wood, and the microfibrillar angle of the wood cell wall may also have an influence on the mechanical properties of the densified wood. The effects of these factors on the performance of the


https://dx.doi.org/10.1021/acsnano.0c07613
ACS Nano 2021, 15, 3646−3673

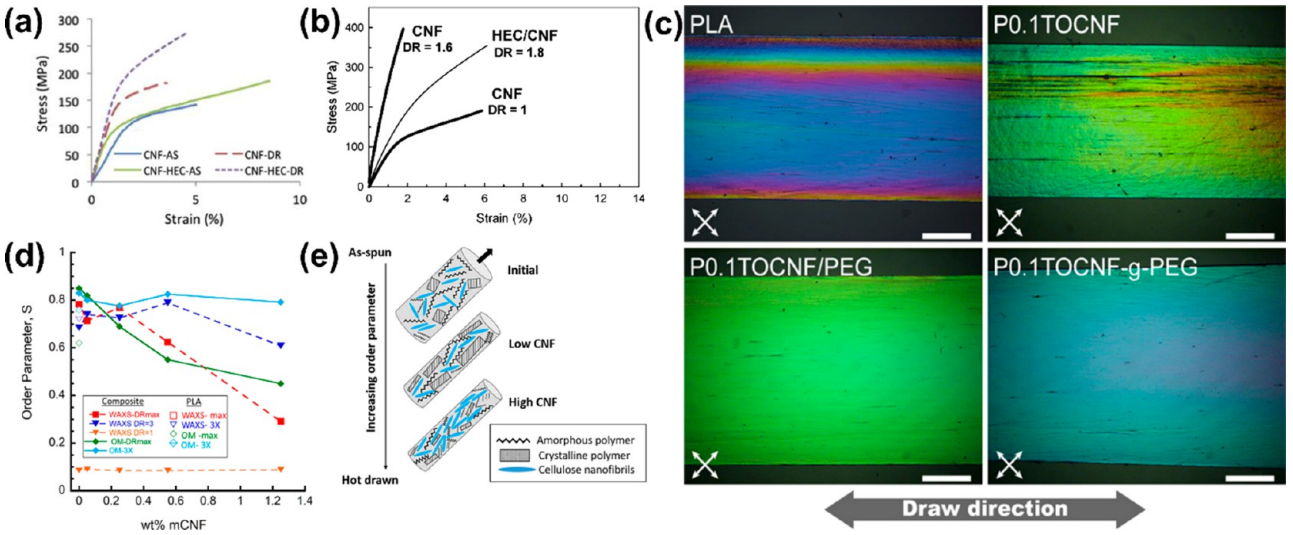


**Figure 8. (a) Stress−strain of as-spun and drawn CNF and HEC/CNF composites. Adapted with permission from ref 62. Copyright 2017 Elsevier. (b) Tensile stress−strain curves of drawn CNF/HEC nanocomposites and reference materials. Adapted with permission from ref 139. Copyright 2012 American Chemical Society. (c) POM images of the surfaces of aligned neat PLA, P0.1TOCNF, P0.1TOCNF/PEG, and P0.1TOCNF-*g*-PEG films (scale bar, 500 μm; directions of the crossed polarizers are shown in the lower left corner). Adapted with permission from ref 46. Copyright 2018 American Chemical Society. (d) Herman's order parameter effect of hot-drawing and mCNF content at a constant PEG content of 5% (dotted lines are unmodified PLA). (e) Visualization of the effect of hot-drawing on fibers with low and high mCNF content. Adapted with permission from ref 80. Copyright 2019 American Chemical Society.**

multifunctional nanocellulose-based materials should call for continued investigation.

## PROPERTIES AND APPLICATIONS OF ALIGNED CELLULOSE NANOFIBERS

**Nanocomposites.** Cellulose nanofibers are being investigated in nanocomposites for a variety of applications, including structural materials.[62,80,138,139,186] The focus for these materials has previously been on isotropic configurations rather than aligned CNFs. However, isotropic and anisotropic CNF composites share some potential benefits. These materials have density (1.5 g/cm$^3$) comparable to those of many engineering polymers and good mechanical properties, which correspond to high specific stiffness or strength. Because of their high aspect ratio, high surface area-to-volume ratio, good stiffness, and strength, CNFs also have potential for mechanical reinforcement in thermosets and thermoplastics, but with concomitant embrittlement in some cases.[80,187,188] However, because CNFs are anisotropic in many of their properties, CNF orientation is expected to affect the properties of CNF nanocomposites, with a higher strength and stiffness in the orientation direction.[14]

Polymer additives such as plasticizers have been added to nanocomposites to help mitigate embrittlement as well as compatibilize nanocelluloses with the polymer matrix. Increased ductility attributable to the addition of polymer additives has enabled larger draw ratios of CNF nanocomposites.[62,80,139] In CNF-matrix composites, this generally coincides with increased orientation.[62,139] For polymer additives such as HEC or PVA, which have hydroxyls in their molecular structure, hydrogen bonding between the matrix and the reinforcement helps ensure good stress transfer despite particle−particle interactions being reduced.[62] Hooshmand *et al.* observed that the modulus and strength of drawn HEC/CNF fibers were 15 ± 2.2 GPa and 260 ± 29 MPa, respectively, compared with 11.3 ± 1.9 GPa modulus and 179 ± 35 MPa strength for drawn neat CNF prepared from the same process (Figure 8a).[62] The authors also observed increased water contact angles for HEC/CNF nanocomposites and inferred that the enhanced hydrophobicity of these nanocomposite might lead to better adhesion in a fiber-reinforced composite such as those made with epoxy.[62] Hydrogel HEC/CNF nanocomposite papers prepared by Sehaqui *et al.* also demonstrated significant improvement in mechanical performance with increasing drawing ratio (Figure 8b).[139] Undrawn nanocomposites exhibited a modulus of 8.2 GPa and tensile strength of 200 MPa, whereas at the maximum drawing ratio, the modulus was 13.3 GPa and the tensile strength was 355 MPa.[139]

Plasticizers in CNF-reinforced composites are also being used to improve CNF dispersion and assist in alignment with the addition of free plasticizer, chemically modifying the CNF surface with the plasticizer, or both.[46,80,138] Plasticized PLA nanocomposites prepared by Singh *et al.* using liquid-assisted extrusion with 1 wt% CNF resulted in increased modulus, strength, elongation at break, and work of fracture compared with the undrawn condition.[138] Likewise, plasticized drawn films exhibited high toughness and ultimate tensile strength with only 0.1 wt% TOCNF or plasticizer-modified TOCNF (TOCNF-*g*-PEG); plasticized materials exhibited superior mechanical properties, higher dispersion, and more homogeneous alignment in POM images of birefringent films (Figure 8c).[46] However, because of the low concentrations of CNFs used in both studies, the alignment of CNFs could not be confirmed in either case but was presumed to follow the polymer orientation. Clarkson *et al.* also demonstrated that melt-spun PLA/mCNF composite fibers with fiber loading up to 1.25 wt% mCNF exhibited improved stiffness with cold-drawing along the fiber axis.[80] However, the alignment of PLA (measured by WAXS and POM) along the tensile axis decreased with increasing CNF content (Figure 8d), despite the overall improvement in polymer order with cold-drawing.[80] A potential reason is that during drawing, as the fiber is


https://dx.doi.org/10.1021/acsnano.0c07613
ACS Nano 2021, 15, 3646−3673

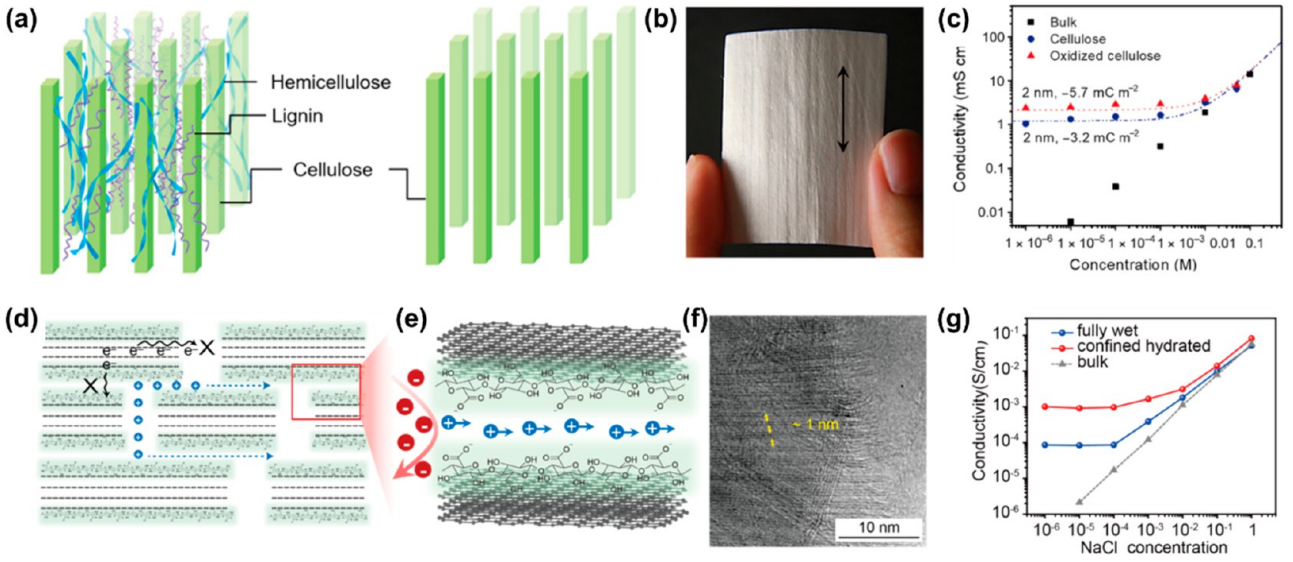


**Figure 9. (a) Schematic of the removal of intertwined lignin and hemicellulose from natural wood to make the nanofluidic membrane. (b) A nanofluidic membrane that inherits the nanofiber alignment direction from natural wood, as marked. (c) Ionic conductivity test with KCl solution for the cellulose membrane before and after oxidization. Reproduced from ref 196 under terms of the CC BY-NC license. Copyright 2019 American Association for the Advancement of Science. (d) Graphite flakes and cellulose fibers are alternately stacked into a layered structure. (e) Debye layers of neighboring graphite flakes overlap to create 2D nanofluidic channels that enable selective ion transport of positive ions. (f) TEM image of the cross-section of a graphite−CNF film in the confined hydrated state with aligned nanoscale channels. (g) Ionic conductivity as a function of electrolyte concentration at different NaCl concentrations. Adapted with permission from ref 197. Copyright 2019 American Chemical Society.**

densifying and alignment is occurring, the formation of a stronger percolation network inhibits the orientation of PLA molecules (Figure 8e). A similar observation was made with cellulose whisker (CW) and PVA nanocomposite fibers, where crystal orientation decreased with increasing CWs concentration; however, the orientation of CWs followed the orientation of the PVA.[189] During cold-drawing, thermoplastic CNF nanocomposites have a chance to undergo further crystallization, and crystal morphology (spherulites vs shish-kebab) can change, which partially accounts for the improvement in mechanical properties. Orientation appears to be a necessity in nanocomposites with small concentrations of CNFs, as little property improvement is observed in isotopically oriented nanocomposites.

**Ion Transport.** Ion transport is crucial for essential functions in living creatures and plays an important role in innovative applications that span energy utilization,[190,191] biosensing,[192] and water treatment.[193] Various materials and structures have been developed for ion transport in diverse devices, such as nanoporous polymer membranes and silicon-based materials, but these materials are not sustainable; they often suffer from the performance degradation upon bending or folding, and the ionic conductivities are limited by the 3D tortuous porous structure.[194,195] Low pore tortuosity is preferred to shorten the transport distance in ionic devices.

Cellulose is an attractive candidate for applications related to fluidic devices. Because the alignment of fibers can be effective in lowering the pore tortuosity, a cellulose membrane composed of aligned nanochannels demonstrated highly efficient and tunable ion regulation.[196] These aligned CNFs are exposed after extraction of intertwined lignin and hemicellulose from the natural wood (Figure 9a). The interface-dominated electrostatic field surrounding the CNFs provides surface charge-governed ion transport along the fiber direction, enabling desirable ionic separation (Figure 9b,c). The long-range ordered arrays of the charged nanofibers led to highly efficient ion transport in the centimeter-long devices. Oxidation treatment has been employed to convert the hydroxy groups to carboxy groups, leading to a more negative zeta potential of −78 mV, which results in a higher ionic conductivity plateau of ∼2 mS $cm^{-1}$ than that of the raw sample (1.1 mS $cm^{-1}$). Another strategy is hybridizing CNFs with 2D materials to construct aligned nanoscale channels through mechanical mixing followed by densification.[197] In a recent study, the 1D CNFs were strongly bonded to the surface of a few layers of 2D graphite flake (Figure 9d,e), assembling into a "brick-and-mortar" stacking laminated structure, in which numerous aligned nanochannels with sizes of 1−1.5 nm were formed between the adjacent cellulose−graphite layers (Figure 9f). As the dimensions of the fluidic channels decrease to as low as the Debye length, the surface charge on the channel walls starts to dominate the ionic behaviors, with only ions of the opposite charge moving through because of electrostatic forces. Governed by this surface charge effect, the ionic conductivity at low salt concentrations (the plateau ionic conductivity at low salt concentrations is ∼1 × $10^{-3}$ S/cm) is significantly higher in nanofluidic channels compared with that of bulk solution (Figure 9g). Cellulose-based materials with aligned nanochannels constructed from two different approaches—top-down fabrication directly from natural wood and bottom-up assembly of cellulose building blocks—offer great opportunities for developing cellulose-based nanofluidic devices. The sustainability of cellulose-based materials is well beyond polymeric materials, while performance reliability issues require continuing efforts.

**Actuators and Sensors.** Recently, a micropatterned soft actuator consisting of a selectively aligned CNF layer and a passivation layer was designed as a high-performance soft actuator.[198] Kuang *et al.* applied a straightforward solvent-


https://dx.doi.org/10.1021/acsnano.0c07613
ACS Nano 2021, 15, 3646−3673

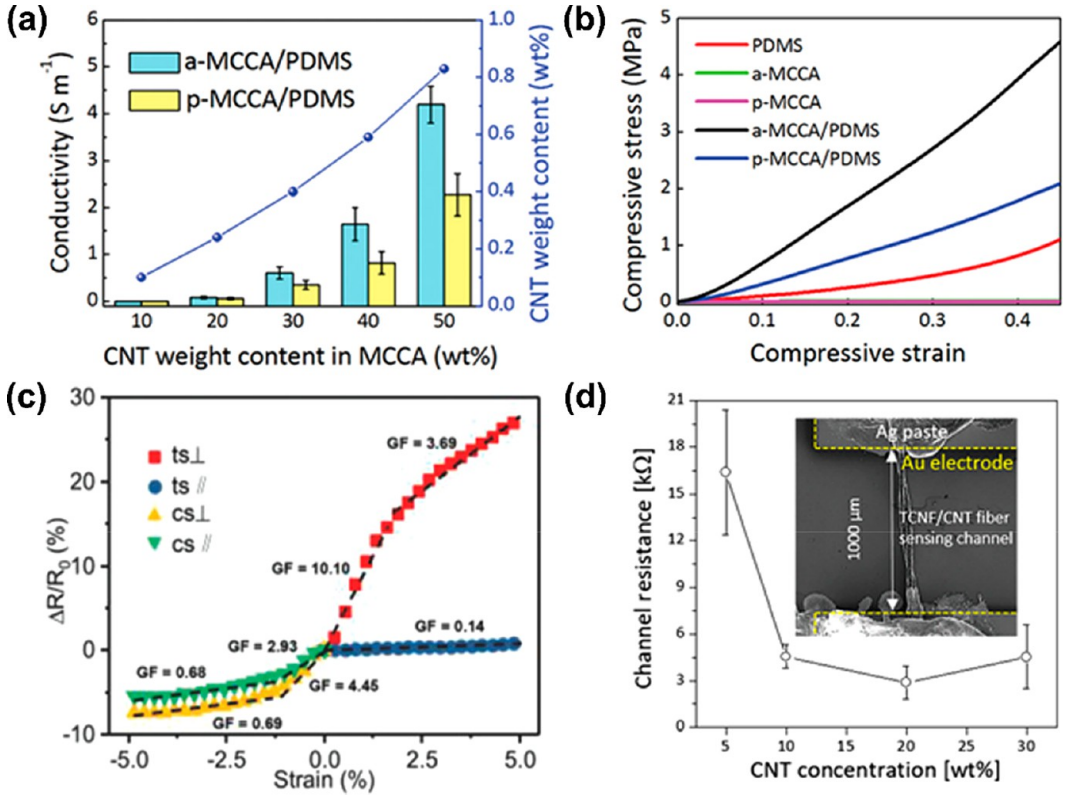


**Figure 10. Aligned CNFs for actuators and sensors. (a) Electric conductivities in two directions of MCCA/PDMS with different CNT weight contents in MCCAs. (b) Compressive stress−strain curves of MCCAs, MCCA/PDMS, and pure PDMS. (Note: the green line is almost covered by the pink line.) Adapted with permission from ref 153. Copyright 2019 Wiley-VCH. (c) Relative resistance changes as a function of strain. Adapted with permission from ref 29. Copyright 2018 Wiley-VCH. (d) Channel resistance variations of the TOCNF/CNT fiber sensing devices with various CNT concentrations. Adapted with permission from ref 200. Copyright 2019 American Chemical Society.**

evaporation-assisted self-assembly method to achieve the desired structure of the CNF layer.[198] Ascribed to the micropatterned structure and disparate hygroscopicity of the CNFs and passivation layers, the resultant CNF actuator demonstrated well-controlled, rapid (response time less than 1 s), and extremely powerful (~1000 times lifting weight ratio) actuation in response to temperature and humidity of the external environment, which is comparable to the best-performing soft actuators reported in the literature. Furthermore, the finite element modeling revealed that the well-aligned CNF layer plays an important role in both the final curvature and generation of the actuation forces. Proof-of-concept demonstrations of the micropatterned soft actuators as mechanical arms and soft walking robots indicate their great potential for soft robots and biomimetic systems.

Moreover, CNFs have the potential to be used to prepare highly sensitive, stretchable, and reversible strain sensors with a 3D hierarchical conductive network structure.[199] Recently, Wang *et al.* prepared an anisotropic microhoneycomb CNF (CellF)-CNT aerogel (denoted MCCA) with unidirectionally aligned penetrating microchannels by a unidirectional freeze-drying method, using the structure-directing function of the CellFs.[153] Because of its anisotropic nature, MCCA-reinforced PDMS (denoted MCCA/PDMS) shows distinct anisotropic behavior. Its electrical conductivity (Figure 10a) and Young's modulus (Figure 10b) along the direction of penetrating microchannels were approximately twice those in the orthogonal direction. MCCA/PDMS is used to make directional strain sensors with electrical resistance as the output signal. A 92% sensitivity difference exists between the microchannel direction and its orthogonal direction. This approach can be used to prepare anisotropic MCCA-based composites with other polymers for different applications. The aligned cellulose fiber also can be added to the carbonized crepe paper (CCP) to fabricate the highly flexible and anisotropic strain sensor.[29] Chen *et al.* put non-conductive crepe cellulose paper into a $N_2$ environment, where it was converted to a conductive carbon fiber network through simple thermal treatment.[29] Meanwhile, its original anisotropic structure is well retained. The fabricated strain sensor based on this CCP exhibits high flexibility, fast response time (<115 ms), high durability (>10 000 cycles), and negligible hysteresis. The CCP strain sensor showed dramatically different gauge factors (10.10 and 0.14, respectively) between tensile bending perpendicular and parallel to the direction of the fibers (Figure 10c). This anisotropic sensing performance was inherited from the crepe paper's anisotropic structure (*i.e.*, aligned cellulose fibers and a corrugated surface), which was well maintained in the CCP. Additionally, the CCP strain sensors had advantages in renewability, low cost, and easy preparation. Chen *et al.* also used CCP strain sensors to direct complex human motions and control a two-degree-of-freedom machine, which indicates the potential applications in multidimensional wearable electronics and smart robots.

Fiber-shaped sensing materials with superior properties can be integrated into smart textiles in various forms by weaving functional components into conventional fabrics. Thus, wearable sensors and electronic textiles based on cellulose


https://dx.doi.org/10.1021/acsnano.0c07613
ACS Nano 2021, 15, 3646−3673

**Table 2. Properties of Aligned CNFs or Composite Fibers Made *via* Spinning and Post-processing Methods**

| composition and fiber content[a] | studied factors[b] | spinning method | fiber diameter ($\mu$m) | orientation index[c] | tensile properties[c] | | | ref |
|---|---|---|---|---|---|---|---|---|
| | | | | | strength (MPa) | modulus (GPa) | strain (%) | |
| CNFs (100%) | SR | dry | ~16 | N/A | 145→220 (↑52%) | N/A | N/A | 136 |
| CNFs (100%) | FC, SS | dry | 207→180 (↓13%) | 0.62→0.65 (↑5%) | 147→198 (↑35%) | 8.3→11.2 (↑35%) | 3.6→3.6 (0%) | 61 |
| CNFs (100%) | additives, DR | dry | 184→130 (↓30%) | 0.49→0.70 (↑43%) | 150→260 (↑73%) | 8.5→15.0 (↑71%) | 5.1→5.7 (↑12%) | 62 |
| TOCNFs (100%) | SS | wet | ~60 | 0.65→0.72 (↑11%) | 90→321 (↑257%) | 8.4→23.6 (↑181%) | 1.5→2.2 (↑47%) | 33 |
| CNFs (100%) | FC | wet | 225→106 (↓53%) | 0.65→0.68 (↑5%) | 136→326 (↑140%) | 8.6→15.5 (↑80%) | 3.7→6.9 (↑86%) | 73 |
| TOCNFs (100%) | SS, SR | wet | ~100 | 0.64→0.73 (↑14%) | 224→294 (↑31%) | 13.1→23.9 (↑82%) | 12.6→4.6 (↓63%) | 45 |
| CNFs (100%) | ECL, D, SS | wet | 59→35 (↓41%) | 0.52→0.61 (↑17%) | 75→155 (↑107%) | 12→22 (↑83%) | ?→11% (−) | 74 |
| TOCNFs (100%) | SS, PRT, D, SR | wet | ~30 | ?→0.86 (−) | 246→543 (↑121%) | 12.6→37.5 (198%) | 11.7→3.7 (↓63%) | 146 |
| TEMPO-BC (100%) | FC, SS, SR, cross-linking | wet | ~50−80 | 0.62→0.72 (↑16%) | 83→357 (↑330%) | 4.2→22.9 (↑433%) | 4.4→2.1 (↓52%) | 75 |
| CNFs/PMMA (4%/96%) | no | electro | ~1−4 | N/A (−) | ?→22 (−) | ?→1.9 (−) | ?→1.2 (−) | 64 |
| CNFs/PEO (21%/79%) | FC | electro | 0.2→0.1 (↓50%) | N/A (−) | ?→17 (−) | ?→0.5 (−) | ?→110 (−) | 93 |

[a]PMMA, poly(methyl methacrylate); PEO, poly(ethylene oxide). [b]SR, stretching ratio; FC, fiber content; SS, spinning speed; DR, drawing ratio; ECL, extrusion capillary length; D, needle diameter; PRT, pre-drying temperature. [c]"→" indicates a property change. The left side of the arrow is the property without the fiber alignment, while the right side of the arrow is the property after the fiber alignment. "?" indicates the values were not reported in the papers. "N/A": not available.

and other fibers were synthesized.[200,201] Cho *et al.* developed a scalable synthesis method (meter scale) for wearable sensing fibers with good mechanical properties and detection performances using nanocellulose/CNT composite fibers.[200] CNFs extracted from tunicate were homogeneously composited with CNTs through wet spinning to produce meter-scale fibers with aligned CNFs. The wearable sensing fibers provided high $NO_2$-sensing performances (resistance change of 0.5% to 0.125 ppm) owing to the rich hydroxyl chemistry, macroporous surfaces, and facile electrical conductivity, even under harsh distortions with tightly knotted and twisted structures (Figure 10d). CNFs were also successfully integrated with a direct weaving process attributable to their superior mechanical flexibility. Additionally, Fu *et al.* described a strain sensor composed of aligned cellulose acetate (CA) nanofibers with belt-like morphology and a reduced graphene oxide (RGO) layer.[201] The spatial alignment, microstructure, and wettability of CA nanofibrous membranes facilitated their close contact with deposited GO colloids. Through a portable and fast hot-pressing process, within 700 s at 150 °C, the GO on CA membranes was facilely reduced to a conductive RGO layer. Moreover, the connection among contiguous CA nanofibers and the interaction between the GO and CA substrate were both highly enhanced, resulting in superior mechanical strength, with Young's modulus of 1.3 GPa and small sheet resistance lower than 10 kΩ. Furthermore, the well-aligned RGO/CA film was sensitive to stretch direction because of partial alignment, which shows us a broad prospect for more electronic textiles.

**Continuous Filaments.** Continuous filaments (fibers) are commonly used for filters, textiles, and composites, and they play an important role in daily life. Fiber-spinning technologies can manufacture continuous filaments from solutions, suspensions, and melts. For cellulose nanofibers, solvent spinning and melt spinning can make cellulose nanofiber-based filaments easily and align cellulose nanofibers to a certain degree at the same time. The properties of filaments made from these different processes are distinct and are affected by process parameters and the alignment of cellulose nanofibers inside the filaments. Additionally, the presence of additives and surface functionalization can affect the alignment process. For instance, in many fiber-spinning alignment processes, the presence of charged groups helps stabilize the aligned cellulose nanofibers.[33,73] Table 2 summarizes properties of cellulose nanofibers or composite filaments aligned *via* spinning and post-processing methods. The authors were unable to identify a study in the literature on melt spinning of CNF−polymer composites with a focus on the CNF alignment. Clarkson *et al.* melt-spun CNF/PEG/PLA composite filaments, emphasizing the alignment of PLA chains.[80] The alignment of CNFs was not detectable by WAXRD, attributed to the low fiber content (1.3 wt%) in the composites, and currently, no other published literature has addressed this challenge.

*Dry Spinning.* Shen *et al.* dry-spun continuous CNF filaments at high velocity on a polyethylene-coated aluminum capstan.[202] The collecting surface was brushed with sunflower oil to create low friction. Such a setting eliminated the need for a coagulation bath or shrinkage control. The CNF suspension was pumped through a nozzle and collected on the capstan. The stretching ratio of the filament was changed by varying the speed of filament spinning and collection. The tensile strength of the filament was maximized at a stretching ratio of 1.7, the highest stretching ratio applied in the study. Hooshmand *et al.* produced CNF filaments from a capillary rheometer.[61] The fiber alignment was tuned by changing the solids content of the CNF suspension and the piston moving rate. Semi-dry filaments were taped on glass sheets to minimize shrinkage. Filaments were air-dried and then oven-dried. The filament


https://dx.doi.org/10.1021/acsnano.0c07613
ACS Nano 2021, 15, 3646−3673

produced using the lowest solids content and highest piston speed produced the best tensile properties. In a later study, Hooshmand *et al.* further enhanced the tensile properties of dry-spun CNF filaments by adding HEC and applying cold drawing.[62] HEC can further stabilize CNF in its suspension, so a suspension of lower solids content is spinnable. Cold drawing was conducted after air drying and before oven drying of the filament using a mechanical tester. A low solids content (4.3 wt %), accompanied with the cold drawing, significantly improved the tensile properties of the dry-spun CNF filaments. The tensile properties of dry-spun CNF filaments without in-line or off-line stretching treatment were at the lower end of reported values, as shown in Table 2.[119]

*Wet Spinning.* Iwamoto *et al.* wet-spun TOCNF (wood pulp-based and tunicate cellulose-based) filaments through an acetone coagulation bath from a suspension having 1 wt% solids content.[33] The alignment of CNFs was achieved by increasing the spinning rate, realized by varying the syringe sizes. Filaments were dried under tension after passing through acetone. Wood-pulp-based CNF filaments had greatly improved tensile properties, particularly when spun at a fast spinning rate. Tensile properties of tunicate-based CNF filaments decreased as the spinning rate and the CNF orientation increased. Besides the spinning rate, the effect of stretching ratio on the tensile properties of wet-spun TOCNF filaments was also studied.[45] The TOCNF suspension was pumped into a $CaCl_2$ coagulation bath using a syringe. The wet filament was soaked in the coagulation bath before being washed, stretched, and dried. A combination of fast spinning rate (10.0 mL/min) and a stretching ratio of 10% resulted in the highest tensile properties of spun TOCNF filaments. Lundahl *et al.* wet-spun CNF suspensions of different solids contents into an acetone bath.[73] The alignment of CNFs increased as the solids content of the suspension decreased. Mohammadi *et al.*[74] explored the effects of extrusion capillary length, diameter, and flow rate on the properties of wet-spun CNF filaments. A CNF suspension with 2 wt% solids content was introduced into an ethanol bath. The wet fiber stayed in the ethanol bath before being dried and collected. Longer capillary length, smaller diameter, and faster flow rate generated a CNF filament with the highest degree of alignment and tensile properties, without compromising toughness. Kim *et al.* studied the effects of four factors[146]—spinning speed, pre-dry temperature, inner diameter of a needle, and stretching ratio—on the tensile properties of wet-spun CNF filaments. A CNF suspension was extruded into a $CaCl_2$ coagulation bath, followed by pre-drying, washing, stretching, and drying. The tensile strength, modulus, and elongation at break of this TOCNF filament, fabricated at a spinning speed of 1700 cm/min, pre-drying temperature of 30 °C, needle inner diameter of 380 $\mu$m, and stretching ratio of 20%, produced the highest values among the reported mechanical property values. A CNF filament was reported to possess high tensile properties (strength of 275 MPa, modulus of 22.5 GPa, and elongation at break of 4%) without any mechanical stretching.[63] Such CNF filaments were produced by pumping the dope through a needle of 1.9 mm diameter and entering into a coagulation bath (*e.g.*, ethanol, dioxane, isopropanol). After a certain soaking time, the wet fibers were removed from the bath and dried at ambient temperature. Because the CNF suspension was produced by a TEMPO treatment, followed by passing through a microfluidizer, such results indicate the importance of starting CNF characteristics on the final filament's mechanical performance. Besides CNFs, BC suspensions were also wet spun into aligned filaments, considering factors such as solids concentration, extrusion rate, cross-linking, and stretching ratio.[75]

*Electrospinning.* Fortunato *et al.* electrospun CNF/poly(ethylene oxide) (PEO) composite filaments from an aqueous suspension.[93] PEO was first dissolved in water, followed by adding various amounts of CNF suspensions. The spinning dope was pumped through a needle. A rotating drum was used to align the electrospun fibers by spinning fast. Investigated CNF contents in PEO were 3.3, 6.5, 11.7, and 21 wt%. Andersson *et al.* proposed a different way for mechanical evaluation of electrospun CNFs/poly(methyl methacrylate) (PMMA) composite filaments with alignment.[64] The spin dope contained CNFs and PMMA in DMF. The fiber alignment was realized by using a rapidly rotating (2000 rpm) cylindrical aluminum drum collector. No comparisons were provided in the mentioned two research papers to illustrate the effect of alignment on the tensile properties of the electrospun CNF/polymer composite filaments. Olsson *et al.* electrospun BC/PMMA composite filaments from their spinning dopes in DMF/THF suspension at proper viscosities.[94] The wet filament was first spun into an aluminum reservoir filled with water. The alignment of electrospun composite filaments was achieved by collecting the filament from the liquid basin over a hollow spool. The purpose of the liquid basin was to support the wet filament, so that a lower collector rotational rate could be applied to align the filament and minimize the filament's stretching and necking at high rotational rates. However, the final filaments picked up defects (kinks) when passing through such a liquid batch.

**Biomedical Applications.** Cellulose materials, including CNFs and BC, are sustainable, biocompatible materials that have been widely used for biomedical and pharmaceutical applications, such as tissue engineering and wound healing.[60,203,204] For these applications, a well-aligned nanofibril arrangement was proven to be beneficial to cell adhesion and direct cell growth.[205] Many types of the cells elongated and aligned parallel to the substrate,[58] and this aligned cell layer was important to initiate cell growth and further develop into a 3D scaffold and form ECMs with an anisotropic architecture. He *et al.* investigated uniaxially aligned electrospun CNF nanocomposites as a scaffold for tissue engineering, and these aligned nanofibers were suitable for human dental follicle cells attachment, which demonstrated the capability to direct cellular organization.[206]

Substrates with patterned morphology, such as an aligned fiber surface, can promote cell alignment and influence the biological response of adherent cell lines on the substrate.[207−210] Elashnikov *et al.* investigated the effect of electrical stimulation on randomly and uniaxially aligned polypyrrole-coated cellulose acetate butyrate nanofibers on the human neuroblastoma cell (SH-SY5Y) and suggested that fiber alignment affected the cell morphology and attachment.[208] A higher degree of fiber alignment resulted in a higher degree of cell orientation. Hua *et al.* investigated the relationship between cell response and surface functionalization of Cladophora nanocellulose (CC) with different functional groups,[209,210] including carboxylated negatively charged CC, hydroxypropyltrimethylammonium-modified positively charged CC, and unmodified CC. The films made from these different CCs have varying fiber alignment, and the carboxylated negatively charged CC (a-CC) had the highest


https://dx.doi.org/10.1021/acsnano.0c07613
ACS Nano 2021, 15, 3646−3673

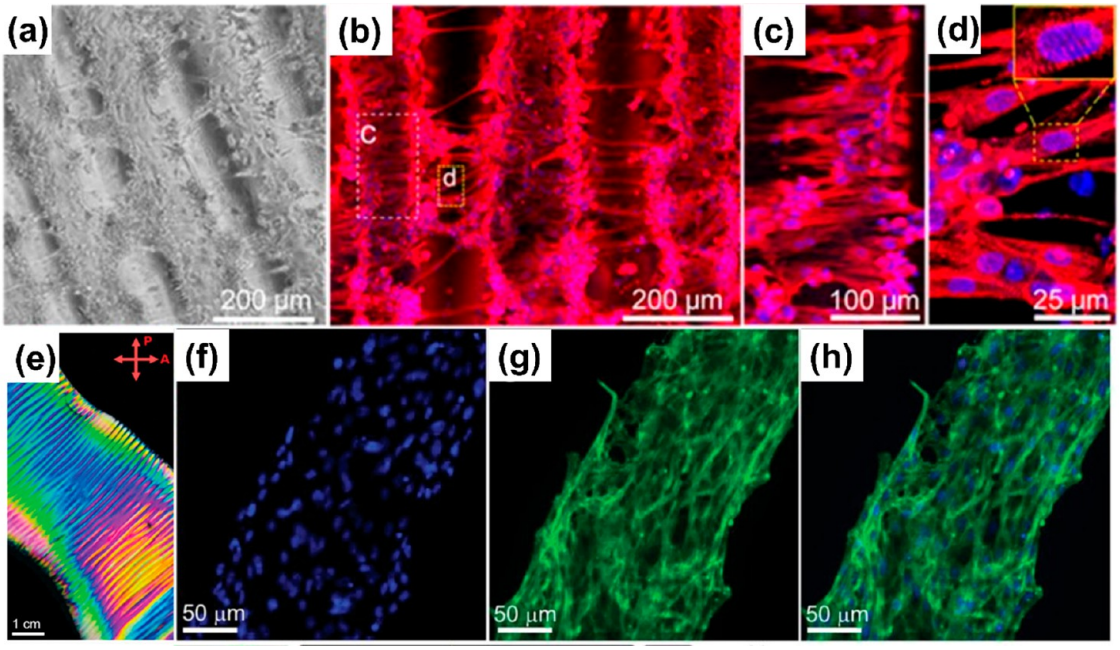


**Figure 11. (a) Bright-field image showing NRVMs cultured on the nanocellulose hydrogels for 5 days. (b–d) Confocal image and corresponding magnified images showing sarcomeric α-actinin in red and nuclei in blue. Adapted with permission from ref 39. Copyright 2018 American Chemical Society. Self-wrinkling cellulose hydrogels induced osteoblast MC3T3 cell alignment. (e) A representative self-wrinkling cellulose hydrogel. (f–h) Bright-field image and fluorescence microscopy images of cells cultured on hydrogel with F-actin stained with fluorescein isothiocyanate-phalloidin (green) and 4′,6-diamidino-2-phenylindole (blue). Adapted with permission from ref 211. Copyright 2019 Wiley-VCH.**

degree of the alignment on the surface. The results suggested that the a-CC film had better cell adhesion and spreading. Similarly, Skogber *et al.* also studied surface functions using plant-based CNF, including unmodified, anionic, and cationic CNFs.[207] An evaporation-induced alignment strategy was used to form a surface with different degrees of alignment. Similar to Hua *et al.*'s results, negative-charged CNF had better fiber alignment and resulted in better cell attachment than positive-charged CNFs and even promoted the cell alignment.

Anisotropic nanocellulose hydrogels with aligned CNFs also serve as good substrates for cell growth to induce cell alignment. Ye *et al.* developed a hydrogel from a cellulose LiOH/urea solution and further induced aligned CNFs by mechanical strength.[39] The obtained hydrogels have anisotropic mechanical properties and optical birefringence and could promote the adhesion and orientation of neonatal rat ventricular myocyte (NRVM). As shown in Figure 11a–d, when NRVMs were cultured on the hydrogel, they attached on the ridge and valley-like region of hydrogel, aligning along the direction of the hydrogel orientation. A similar strategy was also applied to make wrinkled patterned anisotropic hydrogels (Figure 11e) with aligned CNFs for cell alignment. As shown in Figure 11f–h, nearly all of the osteoblast (MC3T3) cells adhered and spread along the ridge-like region on the hydrogel. Fluorescence microscopy images confirmed that the MC3T3 cells adhered and elongated over the ridge-like region in a certain orientation parallel to the linear ridge-like patterns.

**Foams/Aerogels.** The mild conditions used in ice templating make it useful for many applications, including the formation of porous metal oxides, ceramics, scaffolds, and ultra-light-weight polymers (aerogels).[53,151,153,212−215] By far one of the largest applications for ice-templated CNFs, which highlights the importance of aligned CNFs, is in ultra-light-weight, recoverable polymers. These high-performance aerogels feature extremely low densities (around 0.01 g/cm$^3$), high porosity, high elasticity, and recoverable strain. Using the BGF method as described previously, researchers can form anisotropic materials directly with polymer matrices or impregnate synthesized CNF scaffolds with polymer. Mi *et al.* used a hydrophobically modified graphene/CNF aerogel for selective oil uptake.[32] BGF enabled them to synthesize an aerogel with aligned CNF pores and channels for compressibility and sequestration while maintaining porosity for exploitation with chemical vapor deposition to introduce hydrophobicity. Their resultant materials showed recoverable compressibility up to 90% and oil recovery around 85%. Extensive work has been completed to explain why these aligned CNF aerogel structures display such impressive elasticity, despite the known stiffness and strength of CNFs in other materials. Chen *et al.* used BGF to template a cross-linked CNF matrix.[156] Using this simple material, the authors explained that the aligned anisotropic honeycomb structure afforded by BGF of CNFs provides optimal mechanical behavior because of its ability to collapse into a compressible state without true deformation. This was observed using cyclic compressive testing, in which BGF samples showed two distinct regions: a steep linear elastic region and a densification region (Figure 12). A lack of deformation was also confirmed by an almost negligible loss in elasticity. When exposed to the same conditions, comparable samples from UGF or bulk ice templating collapsed.

## CONCLUSIONS AND OUTLOOK

Cellulose nanofibers are emerging sustainable materials for different applications, such as mechanical reinforcement, scaffolds, structural materials, sensors, actuators, and so on.


https://dx.doi.org/10.1021/acsnano.0c07613
ACS Nano 2021, 15, 3646−3673

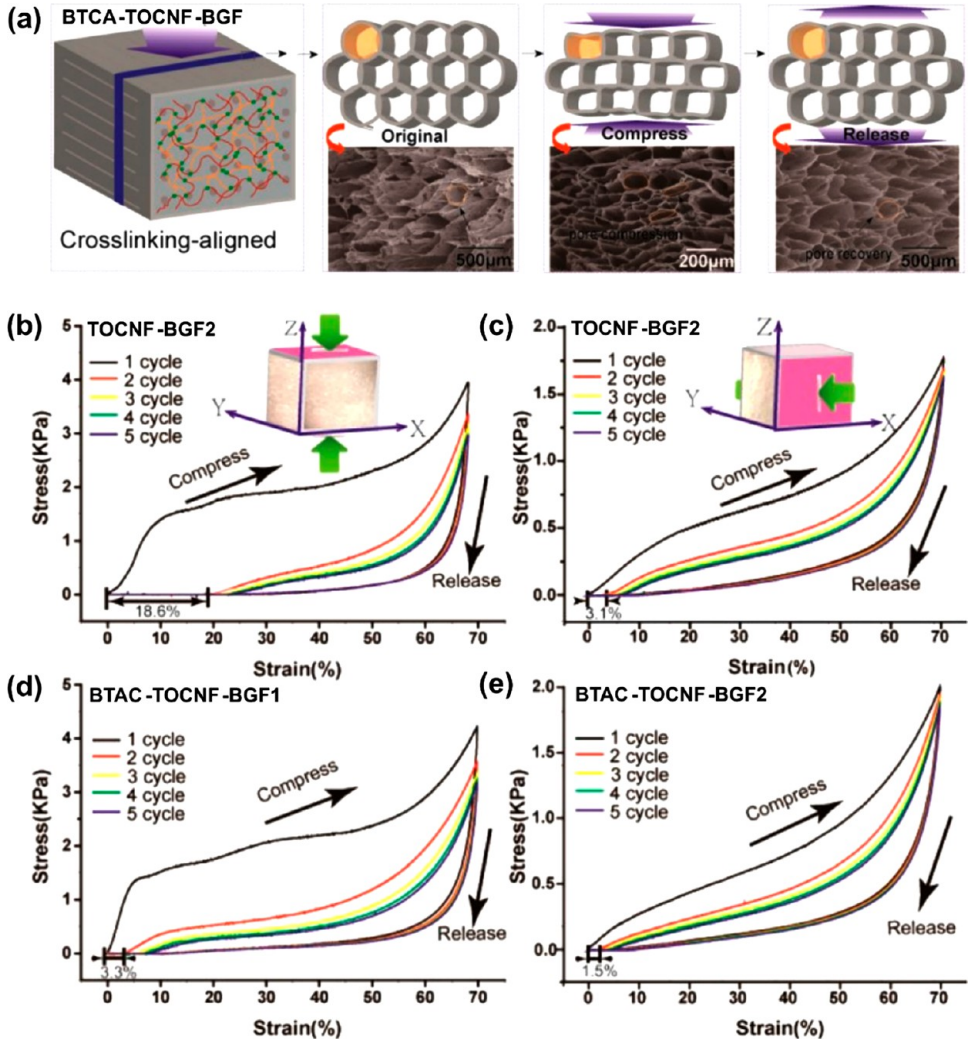


**Figure 12.** (a) Schematic and SEM images of cross-section structure deformation of BGF (BTCA-TOCNF-BGF). The aligned air channels in BGF were not destroyed when lamellar structures were compressed and recovered. Plots of cyclic compressive stress and strain for BGF at a set maximum deformation of 70% for five cycles. The aerogels of (b, c) TOCNF and (d, e) BTCA-TOCNF-BGF modes. The compression direction was perpendicular to the cross-section (XY; panels b, d) and to the ice crystal growth direction (XZ; panels c, e), respectively. Adapted with permission from ref 156. Copyright 2019 American Chemical Society.

The alignment of cellulose nanofibers is important to achieve high-performance cellulose nanofiber-based materials. Exploitation of aligned cellulose nanofibers can serve as a bridge to bring the nanoscale properties of cellulose nanofibers to macroscale enhancement in different applications. However, controlling the alignment of the cellulose nanofibers remains as a big challenge for their application as advanced materials. CNFs and BC are long and flexible, and highly entangled like polymer chains, which makes the alignment of cellulose nanofibers challenging.

Both bottom-up and top-down strategies can align cellulose nanofibers, but the choice of strategies depends on the starting materials and the final applications. For instance, for structural materials, top-down strategies show better performance because of the high degree of the alignment inherited from wood (plants). For gel materials, such as hydrogel, shear and stretching are suitable strategies. Templating is useful for fabricating light-weight anisotropic foams (aerogels). Unfortunately, directly comparing different strategies is difficult due to differences in the methods used to evaluate the alignment. Even though $f_c$ has been widely accepted to quantitatively evaluate the fiber alignment, the value is not reported in many studies. Standardization of the method and evaluation are necessary when the alignment of cellulose nanofibers is discussed to compare different studies. Going forward, a more fundamental understanding of each process is needed to further improve the outcomes of these methods and reveal the underlying laws (*e.g.*, numerical correlations) between processing parameters and properties of the materials. This further understanding includes a more in-depth analysis into the effect of chemical composition on the alignment of cellulose nanofibers. Unfortunately, not all nanocellulose materials contain the same chemical composition, which can greatly affect the alignment process and resultant properties. For instance, residual lignin and hemicellulose present with CNFs can provide stiffness, making it difficult to align the CNFs using certain methods such as foaming, which rely on the flexibility of cellulose nanofibers to achieve optimal results.[216] Additionally, the hydrophobicity of lignin can affect the surface interactions between the cellulose nanofibers and alignment chemistries (*i.e.*, solvents, substrates). Understanding of these variations and their effects on alignment is needed


https://dx.doi.org/10.1021/acsnano.0c07613
ACS Nano 2021, 15, 3646−3673

to improve the success of cellulose nanofiber alignment strategies. Furthermore, scaling up these processes to make aligned cellulose nanofibers at low cost is quite challenging.

Despite the challenges, opportunities exist for further development on the alignment of the cellulose nanofibers, as outlined below.

**Alignment in Cellulose Nanofiber/Polymer Composites.** Cellulose-nanofiber-reinforced polymer composites constitute an important application area for cellulose nanofibers because of their good mechanical properties, low cost, and sustainability. Similar to other fiber-reinforced composites, fiber alignment plays an important role in determining their properties. The top-down strategy has a natural affinity and advantage for manufacturing thermosetting composites. A large portion of the research on cellulose nanofiber/polymer composites focuses on solving the dispersion and compatibility of cellulose nanofibers with the polymer matrix. Unlike the good compatibility between carbon fiber and polymers, cellulose nanofibers are hydrophilic and incompatible with traditional hydrophobic polymers, resulting in aggregation.[11,47] While alignment of the cellulose nanofiber in cellulose nanofiber/polymer composites has been investigated, the potential of the cellulose nanofiber has yet to be fully realized, partially due to the above-mentioned dispersion and compatibility issues. Another challenge for alignment of the cellulose nanofiber in polymer composites arises from the polymer composite manufacturing process. The application of cellulose nanofibers from top-down strategies to thermoplastic composites is challenging due to the compounding difficulty arising from the cellulose nanofiber. Melt processes, such as extrusion, compression, and injection molding, are used for composite processing, during which the alignment of the cellulose nanofiber is challenging. Some alignment during extrusion induced by shear has been observed, but any ordered structure will be disrupted during further manufacturing. The use of a pre-aligned cellulose nanofiber combined with injection molding or extrusion could be one solution, as such processes are compatible with the current industrial practice for producing long fiber-reinforced thermoplastics. Recent advancements in additive manufacturing[217,218] could also create opportunities for aligning cellulose nanofibers in composites through a shear-induced alignment mechanism or continuous fiber-reinforced thermoplastics additive manufacturing.

**Bioinspired Assembly.** Cellulose nanofibers generated in nature can assemble into complicated hierarchical structures with ordered organization. Self-assembly in biological systems provides good examples of diverse structures and process,[219,220] such as nacre, wood, and others. Researchers need to examine how to mimic this natural process to assemble cellulose nanofibers into ordered structures and create high-performance materials. Top-down strategies take the benefit of the natural hierarchical structure of the wood and utilize it in functional materials, where this bioinspired assembly may not be needed. Conversely, for bottom-up strategies to align cellulose nanofibers, the bioinspired assembly could be very useful and offers potential for cellulose nanofiber development. For example, Ahu *et al.* developed a CNC-based chiral reflector through a controlled, bioinspired self-assembly by controlling the water evaporation.[221] However, a fundamental understanding of the biological assembly process and cellulose nanofiber assembly behavior at different length scale is important.

**Simulations.** Although simulation and modeling have been developed in many different areas, more efforts in simulating the alignment process or technologies of cellulose nanofibers are needed. For instance, modeling and simulation of the alignment of cellulose nanofibers[69,88,108,222,223] in a confined flow have been reported in several studies. These data have helped readers gain insight on this flow-induced alignment strategy and how to better design these systems; however, there are no reports for other processes yet. One challenge is that the assembly of cellulose nanofibers involves multiple scales, which is a major challenge for simulations. Recently, Nikolov *et al.* applied *ab initio* and multiscale simulations on chitin assembly to reveal the design principles of high biological composites,[224] which may provide insight for the simulation and modeling of the cellulose nanofiber alignment and assembly. Development on simulations of cellulose nanofiber alignment could help to optimize the alignment process and guide researchers toward developing strategies to achieve better performance.

**Functionalization.** Cellulose nanofibers are decorated with hydroxyls that can easily undergo chemical modifications. Introducing functional groups that can respond to certain external stimuli through chemical modification can help to achieve stimulus-responsive properties and gain the potential to use an external stimulus to align cellulose nanofibers. One example is the carboxyl group on TOCNF, which could be used to induce alignment through tuning of the molecular interactions and realize a self-aligning feature.[92] Kurioz *et al.* reported cinnamate-modified cellulose, which has photo-aligning capability from the anisotropic dimerization of the cinnamates under polarized UV light.[225] Moreover, other functional groups could regulate polymer chains through $\pi-\pi^*$ stacking, hydrogen bonding, and so on and further realize the ordered structures.[226] Additionally, these chemical modifications do not need to be covalent bonds; other bonds, such as hydrogen bonds and ionic bonds, could also be used to introduce responsive groups onto cellulose nanofibers and further improve the alignment of the cellulose nanofibers.

In summary, we believe that with the further advancement of cellulose nanofiber alignment technologies and processes, more functional materials with performance matching that of nanoscale cellulose nanofibers will be developed. The demand for high-performance cellulose nanofiber-based materials will also drive the efforts for large-scale manufacturing of aligned cellulose nanofiber materials.

## AUTHOR INFORMATION


### Corresponding Authors

**Kai Li** − *Chemical Sciences Division, Oak Ridge National Laboratory, Oak Ridge, Tennessee 37831, United States;* orcid.org/0000-0003-1445-3206; Email: lik1@ornl.gov

**Soydan Ozcan** − *Manufacturing Demonstration Facility, Manufacturing Science Division, Oak Ridge National Laboratory, Knoxville, Tennessee 37932, United States;* Email: ozcans@ornl.gov

### Authors

**Caitlyn M. Clarkson** − *Materials and Manufacturing Directorate, Air Force Research Laboratory, Wright-Patterson AFB, Ohio 45433, United States;* orcid.org/0000-0001-9689-0842

**Lu Wang** − *School of Forest Resources and Advanced Structures and Composites Center, University of Maine,*




https://dx.doi.org/10.1021/acsnano.0c07613
*ACS Nano* 2021, 15, 3646−3673

*Orono, Maine 04469, United States;* orcid.org/0000-0002-0458-8011

**Yu Liu** − *Department of Materials Science and Engineering, University of Maryland, College Park, Maryland 20742, United States*

**Meghan Lamm** − *Manufacturing Demonstration Facility, Manufacturing Science Division, Oak Ridge National Laboratory, Knoxville, Tennessee 37932, United States;* orcid.org/0000-0003-3485-4322

**Zhenqian Pang** − *Department of Mechanical Engineering, University of Maryland, College Park, Maryland 20742, United States*

**Yubing Zhou** − *Department of Materials Science and Engineering, University of Maryland, College Park, Maryland 20742, United States*

**Ji Qian** − *Department of Materials Science and Engineering, University of Maryland, College Park, Maryland 20742, United States*

**Mehdi Tajvidi** − *School of Forest Resources and Advanced Structures and Composites Center, University of Maine, Orono, Maine 04469, United States;* orcid.org/0000-0002-3549-1220

**Douglas J. Gardner** − *School of Forest Resources and Advanced Structures and Composites Center, University of Maine, Orono, Maine 04469, United States;* orcid.org/0000-0002-2903-2570

**Halil Tekinalp** − *Manufacturing Demonstration Facility, Manufacturing Science Division, Oak Ridge National Laboratory, Knoxville, Tennessee 37932, United States*

**Liangbing Hu** − *Department of Materials Science and Engineering, University of Maryland, College Park, Maryland 20742, United States;* orcid.org/0000-0002-9456-9315

**Teng Li** − *Department of Mechanical Engineering, University of Maryland, College Park, Maryland 20742, United States;* orcid.org/0000-0001-6252-561X

**Arthur J. Ragauskas** − *Department of Chemical and Biomolecular Engineering, University of Tennessee, Knoxville, Tennessee 37996, United States; Department of Forestry, Wildlife, and Fisheries, Center for Renewable Carbon, The University of Tennessee Institute of Agriculture, Knoxville, Tennessee 37996, United States; UTK-ORNL Joint Institute for Biological Science, Biosciences Division, Oak Ridge National Laboratory, Oak Ridge, Tennessee 37831, United States;* orcid.org/0000-0002-3536-554X

**Jeffrey P Youngblood** − *School of Materials Engineering, Purdue University, West Lafayette, Indiana 47907, United States;* orcid.org/0000-0002-8720-8642

Complete contact information is available at: https://pubs.acs.org/10.1021/acsnano.0c07613

### Notes

The authors declare no competing financial interest.

## ACKNOWLEDGMENTS

This research was supported by the U.S. Department of Energy (DOE), Office of Energy Efficiency and Renewable Energy, Advanced Manufacturing Office, under contract DE-AC05-00OR22725 with UT-Battelle LLC. Authors from University of Maine are grateful for the funding support from UT-Battelle LLC with the U.S. Department of Energy under contract DE-AC05-00OR22725 (subcontract no. 4000174848). Authors at the University of Maryland acknowledge the support of the U.S. National Science Foundation (Grant Nos. 1362256 and 1936452). This manuscript has been authored in part by UT-Battelle, LLC, under contract DE-AC05-00OR22725 with the U.S. DOE. The U.S. government retains and the publisher, by accepting the article for publication, acknowledges that the U.S. government retains a nonexclusive, paid-up, irrevocable, worldwide license to publish or reproduce the published form of this manuscript, or allow others to do so, for U.S. government purposes. DOE will provide public access to these results of federally sponsored research in accordance with the DOE Public Access Plan (http://energy.gov/downloads/doe-public-access-plan).

## VOCABULARY

**Nanocellulose**: Cellulosic materials with one dimension in the nanometer range

**Anisotropic property**: The property of a material which allows it to change or assume different properties in different directions as opposed to isotropy

**Shear force**: Unaligned forces pushing one part of a body in one specific direction, and another part of the body in the opposite direction

**Bottom-up**: The piecing together of systems to give rise to more complex systems, thus making the original systems subsystems of the emergent system

**Top-down**: The breaking down of a system to gain insight into its compositional subsystems in a reverse engineering fashion

## REFERENCES

(1) Fratzl, P.; Weinkamer, R. Nature's Hierarchical Materials. *Prog. Mater. Sci.* **2007**, *52* (8), 1263−1334.

(2) Ling, S.; Kaplan, D. L.; Buehler, M. J. Nanofibrils in Nature and Materials Engineering. *Nat. Rev. Mater.* **2018**, *3* (4), 18016.

(3) Abitbol, T.; Rivkin, A.; Cao, Y.; Nevo, Y.; Abraham, E.; Ben-Shalom, T.; Lapidot, S.; Shoseyov, O. Nanocellulose, a Tiny Fiber with Huge Applications. *Curr. Opin. Biotechnol.* **2016**, *39*, 76−88.

(4) Thomas, B.; Raj, M. C.; B, A. K.; H, R. M.; Joy, J.; Moores, A.; Drisko, G. L.; Sanchez, C. Nanocellulose, a Versatile Green Platform: From Biosources to Materials and Their Applications. *Chem. Rev.* **2018**, *118* (24), 11575−11625.

(5) Zhu, H.; Luo, W.; Ciesielski, P. N.; Fang, Z.; Zhu, J.; Henriksson, G.; Himmel, M. E.; Hu, L. Wood-Derived Materials for Green Electronics, Biological Devices, and Energy Applications. *Chem. Rev.* **2016**, *116* (16), 9305−9374.

(6) Yanamala, N.; Farcas, M. T.; Hatfield, M. K.; Kisin, E. R.; Kagan, V. E.; Geraci, C. L.; Shvedova, A. A. *In Vivo* Evaluation of the Pulmonary Toxicity of Cellulose Nanocrystals: A Renewable and Sustainable Nanomaterial of the Future. *ACS Sustainable Chem. Eng.* **2014**, *2* (7), 1691−1698.

(7) Rajinipriya, M.; Nagalakshmaiah, M.; Robert, M.; Elkoun, S. Importance of Agricultural and Industrial Waste in the Field of Nanocellulose and Recent Industrial Developments of Wood Based Nanocellulose: A Review. *ACS Sustainable Chem. Eng.* **2018**, *6* (3), 2807−2828.

(8) Kim, J.-H.; Shim, B. S.; Kim, H. S.; Lee, Y.-J.; Min, S.-K.; Jang, D.; Abas, Z.; Kim, J. Review of Nanocellulose for Sustainable Future Materials. *Int. J. Pr. Eng. Man.-GT* **2015**, *2* (2), 197−213.

(9) Mohammed, N.; Grishkewich, N.; Tam, K. C. Cellulose Nanomaterials: Promising Sustainable Nanomaterials for Application in Water/Wastewater Treatment Processes. *Environ. Sci.: Nano* **2018**, *5* (3), 623−658.

(10) Khalil, H. A.; Davoudpour, Y.; Saurabh, C. K.; Hossain, M. S.; Adnan, A.; Dungani, R.; Paridah, M.; Sarker, M. Z. I.; Fazita, M. N.; Syakir, M.; Haafiz, M. K. M. A Review on Nanocellulosic Fibres as

New Material for Sustainable Packaging: Process and Applications. *Renewable Sustainable Energy Rev.* **2016**, *64*, 823−836.
(11) Sinquefield, S.; Ciesielski, P. N.; Li, K.; Gardner, D. J.; Ozcan, S. Nanocellulose Dewatering and Drying: Current State and Future Perspectives. *ACS Sustainable Chem. Eng.* **2020**, *8* (26), 9601−9615.
(12) Lamm, M. E.; Li, K.; Qian, J.; Wang, L.; Lavoine, N.; Newman, R.; Gardner, D. J.; Li, T.; Hu, L.; Ragauskas, A. J.; Tekinalp, H.; Kunc, V.; Ozcan, S. Recent Advances in Functional Materials through Nanocellulose Fiber Templating. *Adv. Mater.* **2020**, in press.
(13) Kim, H. C.; Kim, J. W.; Zhai, L.; Kim, J. Strong and Tough Long Cellulose Fibers Made by Aligning Cellulose Nanofibers under Magnetic and Electric Fields. *Cellulose* **2019**, *26* (10), 5821−5829.
(14) Zhu, Q.; Yao, Q.; Sun, J.; Liu, J.; Chen, H.; Xu, W.; Wang, Q. Stimuli Induced Cellulose Nanomaterials Alignment and Its Emerging Applications: A Review. *Carbohydr. Polym.* **2020**, *230*, 115609.
(15) De France, K.; Zeng, Z.; Wu, T.; Nyström, G. Functional Materials from Nanocellulose: Utilizing Structure-Property Relationships in Bottom-Up Fabrication. *Adv. Mater.* **2020**, e2000657.
(16) Habibi, Y.; Lucia, L. A.; Rojas, O. J. Cellulose Nanocrystals: Chemistry, Self-Assembly, and Applications. *Chem. Rev.* **2010**, *110* (6), 3479−3500.
(17) Prathapan, R.; Tabor, R. F.; Garnier, G.; Hu, J. Recent Progress in Cellulose Nanocrystal Alignment and Its Applications. *ACS Applied Bio Materials* **2020**, *3* (4), 1828−1844.
(18) Sugiyama, J.; Chanzy, H.; Maret, G. Orientation of Cellulose Microcrystals by Strong Magnetic Fields. *Macromolecules* **1992**, *25* (16), 4232−4234.
(19) Kimura, F.; Kimura, T.; Tamura, M.; Hirai, A.; Ikuno, M.; Horii, F. Magnetic Alignment of the Chiral Nematic Phase of a Cellulose Microfibril Suspension. *Langmuir* **2005**, *21* (5), 2034−2037.
(20) Souza, S. F.; Mariano, M.; De Farias, M. A.; Bernardes, J. S. Effect of Depletion Forces on the Morphological Structure of Carboxymethyl Cellulose and Micro/Nano Cellulose Fiber Suspensions. *J. Colloid Interface Sci.* **2019**, *538*, 228−236.
(21) Choi, N.; Hur, E.-M.; Kim, S.; Im, S.-K.; Yoon, E. S.; Lee, C. J. Stretching Apparatus and Method for Aligning Microfibrils. US20160152946A1, 2016.
(22) Hird, M. Fluorinated Liquid Crystals−Properties and Applications. *Chem. Soc. Rev.* **2007**, *36* (12), 2070−2095.
(23) Ahadian, S.; Ramon-Azcon, J.; Estili, M.; Liang, X.; Ostrovidov, S.; Shiku, H.; Ramalingam, M.; Nakajima, K.; Sakka, Y.; Bae, H.; Matsue, T.; Khademhosseini, A. Hybrid Hydrogels Containing Vertically Aligned Carbon Nanotubes with Anisotropic Electrical Conductivity for Muscle Myofiber Fabrication. *Sci. Rep.* **2015**, *4*, 4271.
(24) Cowin, S. C. On the Strength Anisotropy of Bone and Wood. *J. Appl. Mech.* **1979**, *46* (4), 832−838.
(25) Zhu, M.; Wang, Y.; Zhu, S.; Xu, L.; Jia, C.; Dai, J.; Song, J.; Yao, Y.; Wang, Y.; Li, Y.; Henderson, D.; Luo, W.; Li, H.; Minus, M. L.; Li, T.; Hu, L. Anisotropic, Transparent Films with Aligned Cellulose Nanofibers. *Adv. Mater.* **2017**, *29* (21), 1606284.
(26) Uetani, K.; Okada, T.; Oyama, H. T. Thermally Conductive and Optically Transparent Flexible Films with Surface-Exposed Nanocellulose Skeletons. *J. Mater. Chem. C* **2016**, *4* (41), 9697−9703.
(27) Uetani, K.; Okada, T.; Oyama, H. T. In-Plane Anisotropic Thermally Conductive Nanopapers by Drawing Bacterial Cellulose Hydrogels. *ACS Macro Lett.* **2017**, *6* (4), 345−349.
(28) Uetani, K.; Okada, T.; Oyama, H. T. Crystallite Size Effect on Thermal Conductive Properties of Nonwoven Nanocellulose Sheets. *Biomacromolecules* **2015**, *16* (7), 2220−2227.
(29) Chen, S.; Song, Y.; Ding, D.; Ling, Z.; Xu, F. Flexible and Anisotropic Strain Sensor Based on Carbonized Crepe Paper with Aligned Cellulose Fibers. *Adv. Funct. Mater.* **2018**, *28* (42), 1802547.
(30) Mredha, M. T. I.; Guo, Y. Z.; Nonoyama, T.; Nakajima, T.; Kurokawa, T.; Gong, J. P. A Facile Method to Fabricate Anisotropic Hydrogels with Perfectly Aligned Hierarchical Fibrous Structures. *Adv. Mater.* **2018**, *30* (9), 1704937.
(31) Mredha, M. T. I.; Le, H. H.; Tran, V. T.; Trtik, P.; Cui, J.; Jeon, I. Anisotropic Tough Multilayer Hydrogels with Programmable Orientation. *Mater. Horiz.* **2019**, *6* (7), 1504−1511.
(32) Mi, H.-Y.; Jing, X.; Politowicz, A. L.; Chen, E.; Huang, H.-X.; Turng, L.-S. Highly Compressible Ultra-Light Anisotropic Cellulose/Graphene Aerogel Fabricated by Bidirectional Freeze Drying for Selective Oil Absorption. *Carbon* **2018**, *132*, 199−209.
(33) Iwamoto, S.; Isogai, A.; Iwata, T. Structure and Mechanical Properties of Wet-Spun Fibers Made from Natural Cellulose Nanofibers. *Biomacromolecules* **2011**, *12* (3), 831−836.
(34) Iwamoto, S.; Kai, W.; Isogai, A.; Iwata, T. Elastic Modulus of Single Cellulose Microfibrils from Tunicate Measured by Atomic Force Microscopy. *Biomacromolecules* **2009**, *10* (9), 2571−2576.
(35) Lahiji, R. R.; Xu, X.; Reifenberger, R.; Raman, A.; Rudie, A.; Moon, R. J. Atomic Force Microscopy Characterization of Cellulose Nanocrystals. *Langmuir* **2010**, *26* (6), 4480−4488.
(36) Li, K.; Skolrood, L.; Aytug, T.; Tekinalp, H.; Ozcan, S. Strong and Tough Cellulose Nanofibrils Composite Films: Mechanism of Synergetic Effect of Hydrogen Bonds and Ionic Interactions. *ACS Sustainable Chem. Eng.* **2019**, *7* (17), 14341−14346.
(37) Saito, T.; Kuramae, R.; Wohlert, J.; Berglund, L. A.; Isogai, A. An Ultrastrong Nanofibrillar Biomaterial: The Strength of Single Cellulose Nanofibrils Revealed *via* Sonication-Induced Fragmentation. *Biomacromolecules* **2013**, *14* (1), 248−253.
(38) Sakurada, I.; Nukushina, Y.; Ito, T. Experimental Determination of the Elastic Modulus of Crystalline Regions in Oriented Polymers. *J. Polym. Sci.* **1962**, *57* (165), 651−660.
(39) Ye, D.; Yang, P.; Lei, X.; Zhang, D.; Li, L.; Chang, C.; Sun, P.; Zhang, L. Robust Anisotropic Cellulose Hydrogels Fabricated *via* Strong Self-Aggregation Forces for Cardiomyocytes Unidirectional Growth. *Chem. Mater.* **2018**, *30* (15), 5175−5183.
(40) Rowell, R. M. *Handbook of Wood Chemistry and Wood Composites*; CRC Press: Boca Raton, FL, 2012.
(41) Diddens, I.; Murphy, B.; Krisch, M.; Müller, M. Anisotropic Elastic Properties of Cellulose Measured Using Inelastic X-Ray Scattering. *Macromolecules* **2008**, *41* (24), 9755−9759.
(42) Song, J.; Chen, C.; Zhu, S.; Zhu, M.; Dai, J.; Ray, U.; Li, Y.; Kuang, Y.; Li, Y.; Quispe, N.; Yao, Y.; Gong, A.; Leiste, U. H.; Bruck, H. A.; Zhu, J. Y.; Vellore, A.; Li, H.; Minus, M. L.; Jia, Z.; Martini, A.; et al. Processing Bulk Natural Wood into a High-Performance Structural Material. *Nature* **2018**, *554* (7691), 224.
(43) Ritchie, R. O. The Conflicts between Strength and Toughness. *Nat. Mater.* **2011**, *10* (11), 817−822.
(44) Magrini, T.; Bouville, F.; Lauria, A.; Le Ferrand, H.; Niebel, T. P.; Studart, A. R. Transparent and Tough Bulk Composites Inspired by Nacre. *Nat. Commun.* **2019**, *10* (1), 2794.
(45) Kafy, A.; Kim, H. C.; Zhai, L.; Kim, J. W.; Hai, L. V.; Kang, T. J.; kim, J. Cellulose Long Fibers Fabricated from Cellulose Nanofibers and Its Strong and Tough Characteristics. *Sci. Rep.* **2017**, *7* (1), 17683.
(46) Geng, S.; Yao, K.; Zhou, Q.; Oksman, K. High-Strength, High-Toughness Aligned Polymer-Based Nanocomposite Reinforced with Ultralow Weight Fraction of Functionalized Nanocellulose. *Biomacromolecules* **2018**, *19* (10), 4075−4083.
(47) Tekinalp, H. L.; Meng, X.; Lu, Y.; Kunc, V.; Love, L. J.; Peter, W. H.; Ozcan, S. High Modulus Biocomposites *via* Additive Manufacturing: Cellulose Nanofibril Networks as "Microsponges. *Composites, Part B* **2019**, *173*, 106817.
(48) Kontturi, E.; Laaksonen, P.; Linder, M. B.; Nonappa; Gröschel, A. H.; Rojas, O. J.; Ikkala, O. Advanced Materials through Assembly of Nanocelluloses. *Adv. Mater.* **2018**, *30* (24), 1703779.
(49) Li, K.; McGrady, D.; Zhao, X.; Ker, D.; Tekinalp, H.; He, X.; Qu, J.; Aytug, T.; Cakmak, E.; Phipps, J.; Ireland, S.; Kunc, V.; Ozcan, S. Surface-Modified and Oven-Dried Microfibrillated Cellulose Reinforced Biocomposites: Cellulose Network Enabled High Performance. *Carbohydr. Polym.* **2021**, *256*, 117525.
(50) Clarkson, C. M.; El Awad Azrak, S. M.; Forti, E. S.; Schueneman, G. T.; Moon, R. J.; Youngblood, J. P. Recent


https://dx.doi.org/10.1021/acsnano.0c07613
*ACS Nano* 2021, 15, 3646−3673

Developments in Cellulose Nanomaterial Composites. *Adv. Mater.* **2020**, e2000718.
(51) Rahman, M. M.; Netravali, A. N. High-Performance Green Nanocomposites Using Aligned Bacterial Cellulose and Soy Protein. *Compos. Sci. Technol.* **2017**, *146*, 183−190.
(52) Oksman, K.; Mathew, A. P.; Sain, M. Novel Bionanocomposites: Processing, Properties and Potential Applications. *Plast., Rubber Compos.* **2009**, *38* (9/10), 396−405.
(53) Nissilä, T.; Hietala, M.; Oksman, K. A Method for Preparing Epoxy-Cellulose Nanofiber Composites with an Oriented Structure. *Composites, Part A* **2019**, *125*, 105515.
(54) Mohammadi, P.; Aranko, A. S.; Landowski, C. P.; Ikkala, O.; Jaudzems, K.; Wagermaier, W.; Linder, M. B. Biomimetic Composites with Enhanced Toughening Using Silk-Inspired Triblock Proteins and Aligned Nanocellulose Reinforcements. *Sci. Adv.* **2019**, *5* (9), eaaw2541.
(55) Diop-Frimpong, B.; Chauhan, V. P.; Krane, S.; Boucher, Y.; Jain, R. K. Losartan Inhibits Collagen I Synthesis and Improves the Distribution and Efficacy of Nanotherapeutics in Tumors. *Proc. Natl. Acad. Sci. U. S. A.* **2011**, *108* (7), 2909−2914.
(56) Lanfer, B.; Seib, F. P.; Freudenberg, U.; Stamov, D.; Bley, T.; Bornhäuser, M.; Werner, C. The Growth and Differentiation of Mesenchymal Stem and Progenitor Cells Cultured on Aligned Collagen Matrices. *Biomaterials* **2009**, *30* (30), 5950−5958.
(57) Li, Y.; Huang, G.; Zhang, X.; Wang, L.; Du, Y.; Lu, T. J.; Xu, F. Engineering Cell Alignment *in Vitro*. *Biotechnol. Adv.* **2014**, *32* (2), 347−365.
(58) Kim, H. N.; Kang, D.-H.; Kim, M. S.; Jiao, A.; Kim, D.-H.; Suh, K.-Y. Patterning Methods for Polymers in Cell and Tissue Engineering. *Ann. Biomed. Eng.* **2012**, *40* (6), 1339−1355.
(59) Tseng, L.-F.; Mather, P. T.; Henderson, J. H. Shape-Memory-Actuated Change in Scaffold Fiber Alignment Directs Stem Cell Morphology. *Acta Biomater.* **2013**, *9* (11), 8790−8801.
(60) Czaja, W. K.; Young, D. J.; Kawecki, M.; Brown, R. M. The Future Prospects of Microbial Cellulose in Biomedical Applications. *Biomacromolecules* **2007**, *8* (1), 1−12.
(61) Hooshmand, S.; Aitomäki, Y.; Norberg, N.; Mathew, A. P.; Oksman, K. Dry-Spun Single-Filament Fibers Comprising Solely Cellulose Nanofibers from Bioresidue. *ACS Appl. Mater. Interfaces* **2015**, *7* (23), 13022−13028.
(62) Hooshmand, S.; Aitomaeki, Y.; Berglund, L.; Mathew, A. P.; Oksman, K. Enhanced Alignment and Mechanical Properties through the Use of Hydroxyethyl Cellulose in Solvent-Free Native Cellulose Spun Filaments. *Compos. Sci. Technol.* **2017**, *150*, 79−86.
(63) Walther, A.; Timonen, J. V. I.; Díez, I.; Laukkanen, A.; Ikkala, O. Multifunctional High-Performance Biofibers Based on Wet-Extrusion of Renewable Native Cellulose Nanofibrils. *Adv. Mater.* **2011**, *23* (26), 2924−2928.
(64) Andersson, R. L.; Salajkova, M.; Mallon, P. E.; Berglund, L. A.; Hedenqvist, M. S.; Olsson, R. T. Micromechanical Tensile Testing of Cellulose-Reinforced Electrospun Fibers Using a Template Transfer Method (TTM). *J. Polym. Environ.* **2012**, *20* (4), 967−975.
(65) Kobe, R.; Iwamoto, S.; Endo, T.; Yoshitani, K.; Teramoto, Y. Stretchable Composite Hydrogels Incorporating Modified Cellulose Nanofiber with Dispersibility and Polymerizability: Mechanical Property Control and Nanofiber Orientation. *Polymer* **2016**, *97*, 480−486.
(66) Gierlinger, N.; Luss, S.; König, C.; Konnerth, J.; Eder, M.; Fratzl, P. Cellulose Microfibril Orientation of Picea Abies and Its Variability at the Micron-Level Determined by Raman Imaging. *J. Exp. Bot.* **2010**, *61* (2), 587−595.
(67) Sun, L.; Singh, S.; Joo, M.; Vega-Sanchez, M.; Ronald, P.; Simmons, B. A.; Adams, P.; Auer, M. Non-Invasive Imaging of Cellulose Microfibril Orientation within Plant Cell Walls by Polarized Raman Microspectroscopy. *Biotechnol. Bioeng.* **2016**, *113* (1), 82−90.
(68) Ye, D.; Cheng, Q.; Zhang, Q.; Wang, Y.; Chang, C.; Li, L.; Peng, H.; Zhang, L. Deformation Drives Alignment of Nanofibers in Framework for Inducing Anisotropic Cellulose Hydrogels with High Toughness. *ACS Appl. Mater. Interfaces* **2017**, *9* (49), 43154−43162.
(69) Mittal, N.; Ansari, F.; Gowda V, K.; Brouzet, C.; Chen, P.; Larsson, P. T.; Roth, S. V.; Lundell, F.; Wågberg, L.; Kotov, N. A.; Söderberg, L. D. Multiscale Control of Nanocellulose Assembly: Transferring Remarkable Nanoscale Fibril Mechanics to Macroscale Fibers. *ACS Nano* **2018**, *12* (7), 6378−6388.
(70) Hakansson, K. M. O.; Fall, A. B.; Lundell, F.; Yu, S.; Krywka, C.; Roth, S. V.; Santoro, G.; Kvick, M.; Prahl Wittberg, L.; Wagberg, L.; Soderberg, L. D. Hydrodynamic Alignment and Assembly of Nanofibrils Resulting in Strong Cellulose Filaments. *Nat. Commun.* **2014**, *5*, 4018.
(71) Uetani, K.; Koga, H.; Nogi, M. Estimation of the Intrinsic Birefringence of Cellulose Using Bacterial Cellulose Nanofiber Films. *ACS Macro Lett.* **2019**, *8* (3), 250−254.
(72) Foster, E. J.; Moon, R. J.; Agarwal, U. P.; Bortner, M. J.; Bras, J.; Camarero-Espinosa, S.; Chan, K. J.; Clift, M. J. D.; Cranston, E. D.; Eichhorn, S. J.; Fox, D. M.; Hamad, W. Y.; Heux, L.; Jean, B.; Korey, M.; Nieh, W.; Ong, K. J.; Reid, M. S.; Renneckar, S.; Roberts, R.; et al. Current Characterization Methods for Cellulose Nanomaterials. *Chem. Soc. Rev.* **2018**, *47* (8), 2609−2679.
(73) Lundahl, M. J.; Cunha, A. G.; Rojo, E.; Papageorgiou, A. C.; Rautkari, L.; Arboleda, J. C.; Rojas, O. J. Strength and Water Interactions of Cellulose I Filaments Wet-Spun from Cellulose Nanofibril Hydrogels. *Sci. Rep.* **2016**, *6* (1), 30695.
(74) Mohammadi, P.; Toivonen, M. S.; Ikkala, O.; Wagermaier, W.; Linder, M. B. Aligning Cellulose Nanofibril Dispersions for Tougher Fibers. *Sci. Rep.* **2017**, *7* (1), 11860.
(75) Yao, J.; Chen, S.; Chen, Y.; Wang, B.; Pei, Q.; Wang, H. Macrofibers with High Mechanical Performance Based on Aligned Bacterial Cellulose Nanofibers. *ACS Appl. Mater. Interfaces* **2017**, *9* (24), 20330−20339.
(76) Kakudo, M.; Kasai, N. *X-Ray Diffraction by Macromolecules*; Kodansha Limited and Springer-Verlag Berlin Heidelberg: Tokyo, Japan, 2005.
(77) Wang, B.; Torres-Rendon, J. G.; Yu, J.; Zhang, Y.; Walther, A. Aligned Bioinspired Cellulose Nanocrystal-Based Nanocomposites with Synergetic Mechanical Properties and Improved Hygromechanical Performance. *ACS Appl. Mater. Interfaces* **2015**, *7* (8), 4595−4607.
(78) Torres-Rendon, J. G.; Schacher, F. H.; Ifuku, S.; Walther, A. Mechanical Performance of Macrofibers of Cellulose and Chitin Nanofibrils Aligned by Wet-Stretching: A Critical Comparison. *Biomacromolecules* **2014**, *15* (7), 2709−2717.
(79) Chowdhury, R. A.; Peng, S. X.; Youngblood, J. Improved Order Parameter (Alignment) Determination in Cellulose Nanocrystal (CNC) Films by a Simple Optical Birefringence Method. *Cellulose* **2017**, *24* (5), 1957−1970.
(80) Clarkson, C. M.; El Awad Azrak, S. M.; Chowdhury, R.; Shuvo, S. N.; Snyder, J.; Schueneman, G.; Ortalan, V.; Youngblood, J. P. Melt Spinning of Cellulose Nanofibril/Polylactic Acid (CNF/PLA) Composite Fibers for High Stiffness. *ACS Appl. Polym. Mater.* **2019**, *1* (2), 160−168.
(81) Ghasemi, S.; Rahimzadeh-Bajgiran, P.; Tajvidi, M.; Shaler, S. M. Birefringence-Based Orientation Mapping of Cellulose Nanofibrils in Thin Films. *Cellulose* **2020**, *27* (2), 677−692.
(82) Jia, C.; Chen, C.; Kuang, Y.; Fu, K.; Wang, Y.; Yao, Y.; Kronthal, S.; Hitz, E.; Song, J.; Xu, F.; Liu, B.; Hu, L. From Wood to Textiles: Top-Down Assembly of Aligned Cellulose Nanofibers. *Adv. Mater.* **2018**, *30* (30), e1801347.
(83) Kim, J.; Chen, Y.; Kang, K.-S.; Park, Y.-B.; Schwartz, M. Magnetic Field Effect for Cellulose Nanofiber Alignment. *J. Appl. Phys.* **2008**, *104* (9), 096104/1−096104/3.
(84) Kimura, F.; Kimura, T. Magnetic Alignment and Patterning of Cellulose Fibers. *Sci. Technol. Adv. Mater.* **2008**, *9* (2), 024212.
(85) Kadimi, A.; Benhamou, K.; Ounaies, Z.; Magnin, A.; Dufresne, A.; Kaddami, H.; Raihane, M. Electric Field Alignment of Nanofibrillated Cellulose (NFC) in Silicone Oil: Impact on Electrical Properties. *ACS Appl. Mater. Interfaces* **2014**, *6* (12), 9418−9425.


https://dx.doi.org/10.1021/acsnano.0c07613
*ACS Nano* 2021, 15, 3646−3673

(86) Xu, S.; Liu, D.; Zhang, Q.; Fu, Q. Electric Field-Induced Alignment of Nanofibrillated Cellulose in Thermoplastic Polyurethane Matrix. *Compos. Sci. Technol.* **2018**, *156*, 117−126.
(87) Chen, Y.; Liu, Y.; Xia, Y.; Liu, X.; Qiang, Z.; Yang, J.; Zhang, B.; Hu, Z.; Wang, Q.; Wu, W.; Duan, Y.; Fu, K. K.; Zhang, J. Electric Field-Induced Assembly and Alignment of Silver-Coated Cellulose for Polymer Composite Films with Enhanced Dielectric Permittivity and Anisotropic Light Transmission. *ACS Appl. Mater. Interfaces* **2020**, *12* (21), 24242−24249.
(88) Rosén, T.; Wang, R.; Zhan, C.; He, H.; Chodankar, S.; Hsiao, B. S. Cellulose Nanofibrils and Nanocrystals in Confined Flow: Single-Particle Dynamics to Collective Alignment Revealed through Scanning Small-Angle X-Ray Scattering and Numerical Simulations. *Phys. Rev. E: Stat. Phys., Plasmas, Fluids, Relat. Interdiscip. Top.* **2020**, *101* (3), 032610.
(89) Rosen, T.; Mittal, N.; Roth, S. V.; Zhang, P.; Soederberg, L. D.; Lundell, F. Dynamic Characterization of Cellulose Nanofibrils in Sheared and Extended Semi-Dilute Dispersions. *arXiv Preprint* **2018**, No. arXiv:1801.07558[cond-mat.soft].
(90) Pahimanolis, N.; Salminen, A.; Penttilä, P. A.; Korhonen, J. T.; Johansson, L.-S.; Ruokolainen, J.; Serimaa, R.; Seppälä, J. Nanofibrillated Cellulose/Carboxymethyl Cellulose Composite with Improved Wet Strength. *Cellulose* **2013**, *20* (3), 1459−1468.
(91) Uetani, K.; Izakura, S.; Kasuga, T.; Koga, H.; Nogi, M. Self-Alignment Sequence of Colloidal Cellulose Nanofibers Induced by Evaporation from Aqueous Suspensions. *Colloids Interfaces* **2018**, *2* (4), 71.
(92) Saito, T.; Uematsu, T.; Kimura, S.; Enomae, T.; Isogai, A. Self-Aligned Integration of Native Cellulose Nanofibrils towards Producing Diverse Bulk Materials. *Soft Matter* **2011**, *7* (19), 8804−8809.
(93) Fortunato, G.; Zimmermann, T.; Lübben, J.; Bordeanu, N.; Hufenus, R. Reinforcement of Polymeric Submicrometer-Sized Fibers by Microfibrillated Cellulose. *Macromol. Mater. Eng.* **2012**, *297* (6), 576−584.
(94) Olsson, R. T.; Kraemer, R.; Lopez-Rubio, A.; Torres-Giner, S.; Ocio, M. J.; Lagarón, J. M. Extraction of Microfibrils from Bacterial Cellulose Networks for Electrospinning of Anisotropic Biohybrid Fiber Yarns. *Macromolecules* **2010**, *43* (9), 4201−4209.
(95) Josefsson, G.; Ahvenainen, P.; Mushi, N. E.; Gamstedt, E. K. Fibril Orientation Redistribution Induced by Stretching of Cellulose Nanofibril Hydrogels. *J. Appl. Phys.* **2015**, *117* (21), 214311.
(96) Baez, C.; Considine, J.; Rowlands, R. Influence of Drying Restraint on Physical and Mechanical Properties of Nanofibrillated Cellulose Films. *Cellulose* **2014**, *21* (1), 347−356.
(97) Chen, Y.; Yang, S.; Fan, D.; Li, G.; Wang, S. Dual-Enhanced Hydrophobic and Mechanical Properties of Long-Range 3D Anisotropic Binary-Composite Nanocellulose Foams *via* Bidirectional Gradient Freezing. *ACS Sustainable Chem. Eng.* **2019**, *7* (15), 12878−12886.
(98) Putra, A.; Kakugo, A.; Furukawa, H.; Gong, J. P.; Osada, Y. Tubular Bacterial Cellulose Gel with Oriented Fibrils on The Curved Surface. *Polymer* **2008**, *49* (7), 1885−1891.
(99) Huang, D.; Wu, J.; Chen, C.; Fu, X.; Brozena, A. H.; Zhang, Y.; Gu, P.; Li, C.; Yuan, C.; Ge, H.; Lu, M.; Zhu, M.; Hu, L.; Chen, Y. Precision Imprinted Nanostructural Wood. *Adv. Mater.* **2019**, *31* (48), e1903270.
(100) Mashkour, M.; Tajvidi, M.; Kimura, T.; Kimura, F.; Ebrahimi, G. Fabricating Unidirectional Magnetic Papers Using Permanent Magnets to Align Magnetic Nanoparticle Covered Natural Cellulose Fibers. *BioResources* **2011**, *6* (4), 4731−4738.
(101) Mashkour, M.; Tajvidi, M.; Kimura, F.; Yousefi, H.; Kimura, T. Strong Highly Anisotropic Magnetocellulose Nanocomposite Films Made by Chemical Peeling and *In Situ* Welding at the Interface Using an Ionic Liquid. *ACS Appl. Mater. Interfaces* **2014**, *6* (11), 8165−8172.
(102) Bordel, D.; Putaux, J.-L.; Heux, L. Orientation of Native Cellulose in an Electric Field. *Langmuir* **2006**, *22* (11), 4899−4901.
(103) Sano, M. B.; Rojas, A. D.; Gatenholm, P.; Davalos, R. V. Electromagnetically Controlled Biological Assembly of Aligned Bacterial Cellulose Nanofibers. *Ann. Biomed. Eng.* **2010**, *38* (8), 2475−84.
(104) Yan, L.; Jia, S. R.; Zheng, X. T.; Zhong, C.; Liu, M.; Xu, G. J. The Effect of Growth, Migration and Bacterial Cellulose Synthesis of Gluconacetobacter Xylinus in Presence of Direct Current Electric Field Condition. *Adv. Mater. Res.* **2012**, *550*, 1108−1113.
(105) Bajpai, P. Brief Description of the Pulp and Papermaking Process. In *Biotechnology for Pulp and Paper Processing*; Springer Singapore: The Gateway West, Singapore, 2018; pp 9−26.
(106) Mittal, N.; Benselfelt, T.; Ansari, F.; Gordeyeva, K.; Roth, S. V.; Wågberg, L.; Söderberg, L. D. Ion-Specific Assembly of Strong, Tough, and Stiff Biofibers. *Angew. Chem., Int. Ed.* **2019**, *58* (51), 18562−18569.
(107) Rosen, T.; Brouzet, C.; Roth, S. V.; Lundell, F.; Soederberg, L. D. Evaluating Alignment of Elongated Nanoparticles in Cylindrical Geometries through Small Angle X-Ray Scattering Experiments. *arXiv Preprint* **2017**, No. arXiv:1711.02489[cond-mat.soft].
(108) Rosén, T.; Brouzet, C.; Roth, S. V.; Lundell, F.; Söderberg, L. D. Three-Dimensional Orientation of Nanofibrils in Axially Symmetric Systems Using Small-Angle X-Ray Scattering. *J. Phys. Chem. C* **2018**, *122* (12), 6889−6899.
(109) Luo, H.; Li, W.; Yang, Z.; Ao, H.; Xiong, G.; Zhu, Y.; Tu, J.; Wan, Y. Preparation of Oriented Bacterial Cellulose Nanofibers by Flowing Medium-Assisted Biosynthesis and Influence of Flowing Velocity. *J. Polym. Eng.* **2018**, *38* (3), 299−305.
(110) Wan, Y.; Hu, D.; Xiong, G.; Li, D.; Guo, R.; Luo, H. Directional Fluid Induced Self-Assembly of Oriented Bacterial Cellulose Nanofibers for Potential Biomimetic Tissue Engineering Scaffolds. *Mater. Chem. Phys.* **2015**, *149*, 7−11.
(111) Krystynowicz, A.; Czaja, W.; Wiktorowska-Jezierska, A.; Gonçalves-Miśkiewicz, M.; Turkiewicz, M.; Bielecki, S. Factors Affecting the Yield and Properties of Bacterial Cellulose. *J. Ind. Microbiol. Biotechnol.* **2002**, *29* (4), 189−195.
(112) Chowdhury, R. A.; Clarkson, C.; Apalangya, V. A.; Islam, S. N.; Youngblood, J. P. Roll-to-Roll Fabrication of Cellulose Nanocrystal-Poly (Vinyl Alcohol) Composite Coatings with Controlled Anisotropy. *Cellulose* **2018**, *25* (11), 6547−6560.
(113) Kumar, V.; Elfving, A.; Koivula, H.; Bousfield, D.; Toivakka, M. Roll-to-Roll Processed Cellulose Nanofiber Coatings. *Ind. Eng. Chem. Res.* **2016**, *55* (12), 3603−3613.
(114) Chowdhury, R. A.; Nuruddin, M. D.; Clarkson, C.; Montes, F.; Howarter, J.; Youngblood, P. J. Cellulose Nanocrystal (CNC) Coatings with Controlled Anisotropy as High-Performance Gas Barrier Films. *ACS Appl. Mater. Interfaces* **2019**, *11* (11), 1376−1383.
(115) Uetani, K.; Yano, H. Self-Organizing Capacity of Nanocelluloses *via* Droplet Evaporation. *Soft Matter* **2013**, *9* (12), 3396−3401.
(116) Clemons, C. Nanocellulose in Spun Continuous Fibers: A Review and Future Outlook. *J. Renew. Mater.* **2016**, *4* (5), 327−339.
(117) Lundahl, M. J.; Klar, V.; Wang, L.; Ago, M.; Rojas, O. J. Spinning of Cellulose Nanofibrils into Filaments: A Review. *Ind. Eng. Chem. Res.* **2017**, *56* (1), 8−19.
(118) Lu, H.-C.; Kao, S.-Y.; Yu, H.-F.; Chang, T.-H.; Kung, C.-W.; Ho, K.-C. Achieving Low-Energy Driven Viologens-Based Electrochromic Devices Utilizing Polymeric Ionic Liquids. *ACS Appl. Mater. Interfaces* **2016**, *8* (44), 30351−30361.
(119) Ghasemi, S.; Tajvidi, M.; Bousfield, D. W.; Gardner, D. J.; Gramlich, W. M. Dry-Spun Neat Cellulose Nanofibril Filaments: Influence of Drying Temperature and Nanofibril Structure on Filament Properties. *Polymers* **2017**, *9* (9), 392.
(120) Ghasemi, S.; Tajvidi, M.; Gardner, D. J.; Bousfield, D. W.; Shaler, S. M. Effect of Wettability and Surface Free Energy of Collection Substrates on the Structure and Morphology of Dry-Spun Cellulose Nanofibril Filaments. *Cellulose* **2018**, *25* (11), 6305−6317.
(121) Chen, S.; Schueneman, G.; Pipes, R. B.; Youngblood, J.; Moon, R. J. Effects of Crystal Orientation on Cellulose Nanocrystals−


https://dx.doi.org/10.1021/acsnano.0c07613
*ACS Nano* 2021, 15, 3646−3673

Cellulose Acetate Nanocomposite Fibers Prepared by Dry Spinning. *Biomacromolecules* **2014**, *15* (10), 3827−3835.
(122) Rezaei, A.; Nasirpour, A.; Fathi, M. Application of Cellulosic Nanofibers in Food Science Using Electrospinning and Its Potential Risk. *Compr. Rev. Food Sci. Food Saf.* **2015**, *14* (3), 269−284.
(123) Hooshmand, S.; Aitomäki, Y.; Skrifvars, M.; Mathew, A. P.; Oksman, K. All-Cellulose Nanocomposite Fibers Produced by Melt Spinning Cellulose Acetate Butyrate and Cellulose Nanocrystals. *Cellulose* **2014**, *21* (4), 2665−2678.
(124) Sanders, J. E.; Han, Y.; Rushing, T. S.; Gardner, D. J. Electrospinning of Cellulose Nanocrystal-Filled Poly (Vinyl Alcohol) Solutions: Material Property Assessment. *Nanomaterials* **2019**, *9* (5), 805.
(125) Huang, Z.-M.; Zhang, Y.-Z.; Kotaki, M.; Ramakrishna, S. A Review on Polymer Nanofibers by Electrospinning and Their Applications in Nanocomposites. *Compos. Sci. Technol.* **2003**, *63* (15), 2223−2253.
(126) Wang, X.; Wang, L.; Wu, Q.; Bao, F.; Yang, H.; Qiu, X.; Chang, J. Chitosan/Calcium Silicate Cardiac Patch Stimulates Cardiomyocyte Activity and Myocardial Performance after Infarction by Synergistic Effect of Bioactive Ions and Aligned Nanostructure. *ACS Appl. Mater. Interfaces* **2019**, *11* (1), 1449−1468.
(127) Li, K.; McGuire, M.; Lupini, A.; Skolrood, L.; List, F.; Ozpineci, B.; Ozcan, S.; Aytug, T. Copper−Carbon Nanotube Composites Enabled by Electrospinning for Advanced Conductors. *ACS Applied Nano Materials* **2020**, *3* (7), 6863−6875.
(128) Xue, J.; Wu, T.; Dai, Y.; Xia, Y. Electrospinning and Electrospun Nanofibers: Methods, Materials, and Applications. *Chem. Rev.* **2019**, *119* (8), 5298−5415.
(129) Yang, Z.; Si, J.; Cui, Z.; Ye, J.; Wang, X.; Wang, Q.; Peng, K.; Chen, W.; Chen, S.-C. Biomimetic Composite Scaffolds Based on Surface Modification of Polydopamine on Electrospun Poly(Lactic Acid)/Cellulose Nanofibrils. *Carbohydr. Polym.* **2017**, *174*, 750−759.
(130) Kim, C.-W.; Kim, D.-S.; Kang, S.-Y.; Marquez, M.; Joo, Y. L. Structural Studies of Electrospun Cellulose Nanofibers. *Polymer* **2006**, *47* (14), 5097−5107.
(131) Frey, M. W. Electrospinning Cellulose and Cellulose Derivatives. *Polym. Rev.* **2008**, *48* (2), 378−391.
(132) Gindl, W.; Emsenhuber, G.; Maier, G.; Keckes, J. Cellulose in Never-Dried Gel Oriented by an AC Electric Field. *Biomacromolecules* **2009**, *10* (5), 1315−1318.
(133) Li, K.; Choudhary, H.; Rogers, R. D. Ionic Liquids for Sustainable Processes: Liquid Metal Catalysis. *Curr. Opin. Green Sustain. Chem.* **2018**, *11*, 15−21.
(134) Ye, D.; Lei, X.; Li, T.; Cheng, Q.; Chang, C.; Hu, L.; Zhang, L. Ultrahigh Tough, Super Clear, and Highly Anisotropic Nanofiber-Structured Regenerated Cellulose Films. *ACS Nano* **2019**, *13* (4), 4843−4853.
(135) Zhu, R.; Yadama, V.; Liu, H.; Lin, R. J.; Harper, D. P. Fabrication and Characterization of Nylon 6/Cellulose Nanofibrils Melt-Spun Nanocomposite Filaments. *Composites, Part A* **2017**, *97*, 111−119.
(136) John, M. J.; Anandjiwala, R.; Oksman, K.; Mathew, A. P. Melt-Spun Polylactic Acid Fibers: Effect of Cellulose Nanowhiskers on Processing and Properties. *J. Appl. Polym. Sci.* **2013**, *127* (1), 274−281.
(137) Blaker, J. J.; Lee, K.-Y.; Walters, M.; Drouet, M.; Bismarck, A. Aligned Unidirectional PLA/Bacterial Cellulose Nanocomposite Fibre Reinforced PDLLA Composites. *React. Funct. Polym.* **2014**, *85*, 185−192.
(138) Singh, A. A.; Geng, S.; Herrera, N.; Oksman, K. Aligned Plasticized Polylactic Acid Cellulose Nanocomposite Tapes: Effect of Drawing Conditions. *Composites, Part A* **2018**, *104*, 101−107.
(139) Sehaqui, H.; Ezekiel Mushi, N.; Morimune, S.; Salajkova, M.; Nishino, T.; Berglund, L. A. Cellulose Nanofiber Orientation in Nanopaper and Nanocomposites by Cold Drawing. *ACS Appl. Mater. Interfaces* **2012**, *4* (2), 1043−1049.
(140) Wang, S.; Jiang, F.; Xu, X.; Kuang, Y.; Fu, K.; Hitz, E.; Hu, L. Super-Strong, Super-Stiff Macrofibers with Aligned, Long Bacterial Cellulose Nanofibers. *Adv. Mater.* **2017**, *29* (35), 1702498.
(141) Takagi, H.; Nakagaito, A. N.; Sakaguchi, Y. Structural Modification of Cellulose Nanocomposites by Stretching. *WIT Trans. Eng. Sci.* **2017**, *116*, 251−256.
(142) Frank, E.; Ingildeev, D.; Buchmeiser, M. R. High-Performance PAN-Based Carbon Fibers and Their Performance Requirements. In *Structure and Properties of High-Performance Fibers*; Bhat, G., Ed.; Elsevier Ltd.: Amsterdam, The Netherlands, 2017; pp 7−30.
(143) Murase, Y.; Nagai, A. Melt Spinning. In *Advanced Fiber Spinning Technology*; Woodhead Publishing: Oxford, UK, 1994; pp 25−64.
(144) Katayama, K.-i.; Tsuji, M. Fundamentals of Spinning. In *Advanced Fiber Spinning Technology*; Nakajima, T., Kajiwara, K., McIntyre, J. E., Eds.; Woodhead Publishing: Oxford, UK, 1994; pp 1−24.
(145) Yang, H. H.; Allen, S. R. Fiber Spinning of Anisotropic Polymers. In *Advanced Fiber Spinning Technology*; Nakajima, T., Kajiwara, K., McIntyre, J. E., Eds.; Woodhead Publishing: Oxford, UK, 1994; pp 130−159.
(146) Kim, H. C.; Kim, D.; Lee, J. Y.; Zhai, L.; Kim, J. Effect of Wet Spinning and Stretching to Enhance Mechanical Properties of Cellulose Nanofiber Filament. *Int. J. Pr. Eng. Man.-GT* **2019**, *6* (3), 567−575.
(147) Tang, H.; Butchosa, N.; Zhou, Q. A Transparent, Hazy, and Strong Macroscopic Ribbon of Oriented Cellulose Nanofibrils Bearing Poly(Ethylene Glycol). *Adv. Mater.* **2015**, *27* (12), 2070−2076.
(148) Shahbazi, M.-A.; Ghalkhani, M.; Maleki, H. Directional Freeze-Casting: A Bioinspired Method to Assemble Multifunctional Aligned Porous Structures for Advanced Applications. *Adv. Eng. Mater.* **2020**, *22*, 2000033.
(149) Lavoine, N.; Bergström, L. Nanocellulose-Based Foams and Aerogels: Processing, Properties, and Applications. *J. Mater. Chem. A* **2017**, *5* (31), 16105−16117.
(150) Cheng, Q.; Huang, C.; Tomsia, A. P. Freeze Casting for Assembling Bioinspired Structural Materials. *Adv. Mater.* **2017**, *29* (45), 1703155.
(151) Zhang, X.; Liu, M.; Wang, H.; Yan, N.; Cai, Z.; Yu, Y. Ultralight, Hydrophobic, Anisotropic Bamboo-Derived Cellulose Nanofibrils Aerogels with Excellent Shape Recovery *via* Freeze-Casting. *Carbohydr. Polym.* **2019**, *208*, 232−240.
(152) Han, J.; Zhou, C.; Wu, Y.; Liu, F.; Wu, Q. Self-Assembling Behavior of Cellulose Nanoparticles during Freeze-Drying: Effect of Suspension Concentration, Particle Size, Crystal Structure, and Surface Charge. *Biomacromolecules* **2013**, *14* (5), 1529−1540.
(153) Wang, C.; Pan, Z.-Z.; Lv, W.; Liu, B.; Wei, J.; Lv, X.; Luo, Y.; Nishihara, H.; Yang, Q.-H. A Directional Strain Sensor Based on Anisotropic Microhoneycomb Cellulose Nanofiber-Carbon Nanotube Hybrid Aerogels Prepared by Unidirectional Freeze Drying. *Small* **2019**, *15*, 1805363.
(154) Munier, P.; Gordeyeva, K.; Bergstroem, L.; Fall, A. B. Directional Freezing of Nanocellulose Dispersions Aligns the Rod-Like Particles and Produces Low-Density and Robust Particle Networks. *Biomacromolecules* **2016**, *17* (5), 1875−1881.
(155) Liang, L.; Huang, C.; Hao, N.; Ragauskas, A. J. Cross-Linked Poly(Methyl Vinyl Ether-*co*-Maleic Acid)/Poly(Ethylene Glycol)/Nanocellulosics Foams *via* Directional Freezing. *Carbohydr. Polym.* **2019**, *213*, 346−351.
(156) Chen, Y.; Fan, D.; Lyu, S.; Li, G.; Jiang, F.; Wang, S. Elasticity-Enhanced and Aligned Structure Nanocellulose Foam-Like Aerogel Assembled with Cooperation of Chemical Art and Gradient Freezing. *ACS Sustainable Chem. Eng.* **2019**, *7* (1), 1381−1388.
(157) Gutiérrez, M. C.; Ferrer, M. L.; del Monte, F. Ice-Templated Materials: Sophisticated Structures Exhibiting Enhanced Functionalities Obtained after Unidirectional Freezing and Ice-Segregation-Induced Self-Assembly. *Chem. Mater.* **2008**, *20* (3), 634−648.


https://dx.doi.org/10.1021/acsnano.0c07613
*ACS Nano* 2021, 15, 3646−3673

(158) Putra, A.; Kakugo, A.; Furukawa, H.; Gong, J. P.; Osada, Y.; Uemura, T.; Yamamoto, M. Production of Bacterial Cellulose with Well Oriented Fibril on PDMS Substrate. *Polym. J.* **2008**, *40* (2), 137−142.
(159) Kondo, T.; Nojiri, M.; Hishikawa, Y.; Togawa, E.; Romanovicz, D.; Brown, R. M. Biodirected Epitaxial Nanodeposition of Polymers on Oriented Macromolecular Templates. *Proc. Natl. Acad. Sci. U. S. A.* **2002**, *99* (22), 14008−14013.
(160) Tomita, Y.; Kondo, T. Influential Factors to Enhance the Moving Rate of Acetobacter Xylinum Due to Its Nanofiber Secretion on Oriented Templates. *Carbohydr. Polym.* **2009**, *77* (4), 754−759.
(161) Kondo, T.; Togawa, E.; Brown, R. M. "Nematic Ordered Cellulose": A Concept of Glucan Chain Association. *Biomacromolecules* **2001**, *2* (4), 1324−1330.
(162) Togawa, E.; Kondo, T. Change of Morphological Properties in Drawing Water-Swollen Cellulose Films Prepared from Organic Solutions. A View of Molecular Orientation in the Drawing Process. *J. Polym. Sci., Part B: Polym. Phys.* **1999**, *37* (5), 451−459.
(163) Kondo, T.; Kasai, W.; Brown, R. M. Formation of Nematic Ordered Cellulose and Chitin. *Cellulose* **2004**, *11* (3−4), 463−474.
(164) Kondo, T.; Kasai, W.; Nojiri, M.; Hishikawa, Y.; Togawa, E.; Romanovicz, D.; Brown, R. M., Jr Regulated Patterns of Bacterial Movements Based on Their Secreted Cellulose Nanofibers Interacting Interfacially with Ordered Chitin Templates. *J. Biosci. Bioeng* **2012**, *114* (1), 113−120.
(165) Sjostrom, E. *Wood Chemistry: Fundamentals and Applications*, 2nd ed.; Academic Press: San Diego, CA, 1993.
(166) Berglund, L. A.; Burgert, I. Bioinspired Wood Nanotechnology for Functional Materials. *Adv. Mater.* **2018**, *30* (19), 1704285.
(167) Agarwal, U. P. Raman Imaging to Investigate Ultrastructure and Composition of Plant Cell Walls: Distribution of Lignin and Cellulose in Black Spruce Wood (Picea Mariana). *Planta* **2006**, *224* (5), 1141.
(168) Adler, D. C.; Buehler, M. J. Mesoscale Mechanics of Wood Cell Walls under Axial Strain. *Soft Matter* **2013**, *9* (29), 7138−7144.
(169) Fang, Z.; Li, B.; Liu, Y.; Zhu, J.; Li, G.; Hou, G.; Zhou, J.; Qiu, X. Critical Role of Degree of Polymerization of Cellulose in Super-Strong Nanocellulose Films. *Matter-Us* **2020**, *2* (4), 1000−1014.
(170) Erickson, E. *Mechanical Properties of Laminated Modified Wood*; Forest Service, U.S. Department of Agriculture, Madison, WI, 1965.
(171) Fang, C.-H.; Mariotti, N.; Cloutier, A.; Koubaa, A.; Blanchet, P. Densification of Wood Veneers by Compression Combined with Heat and Steam. *Eur. J. Wood Wood Prod.* **2012**, *70* (1−3), 155−163.
(172) Bekhta, P.; Hiziroglu, S.; Shepelyuk, O. Properties of Plywood Manufactured from Compressed Veneer as Building Material. *Mater. Eng.* **2009**, *30* (4), 947−953.
(173) Kultikova, E. V. Structure and Properties Relationships of Densified Wood. Doctoral Thesis, Virginia Tech, 1999.
(174) Gong, M.; Lamason, C.; Li, L. Interactive Effect of Surface Densification and Post-Heat-Treatment on Aspen Wood. *J. Mater. Process. Technol.* **2010**, *210* (2), 293−296.
(175) Hill, C. A.; Ramsay, J.; Keating, B.; Laine, K.; Rautkari, L.; Hughes, M.; Constant, B. The Water Vapour Sorption Properties of Thermally Modified and Densified Wood. *J. Mater. Sci.* **2012**, *47* (7), 3191−3197.
(176) Laine, K.; Segerholm, K.; Wålinder, M.; Rautkari, L.; Hughes, M. Wood Densification and Thermal Modification: Hardness, Set-Recovery and Micromorphology. *Wood Sci. Technol.* **2016**, *50* (5), 883−894.
(177) Pařil, P.; Brabec, M.; Maňák, O.; Rousek, R.; Rademacher, P.; Čermák, P.; Dejmal, A. Comparison of Selected Physical and Mechanical Properties of Densified Beech Wood Plasticized by Ammonia and Saturated Steam. *Eur. J. Wood Wood Prod.* **2014**, *72* (5), 583−591.
(178) Chen, C. J.; Kuang, Y. D.; Zhu, S. Z.; Burgert, I.; Keplinger, T.; Gong, A.; Li, T.; Berglund, L.; Eichhorn, S. J.; Hu, L. B. Structure-Property-Function Relationships of Natural and Engineered Wood. *Nat. Rev. Mater.* **2020**, *5* (9), 642−666.
(179) Jia, C.; Li, T.; Chen, C.; Dai, J.; Kierzewski, I. M.; Song, J.; Li, Y.; Yang, C.; Wang, C.; Hu, L. Scalable, Anisotropic Transparent Paper Directly from Wood for Light Management in Solar Cells. *Nano Energy* **2017**, *36*, 366−373.
(180) Li, T.; Zhai, Y.; He, S.; Gan, W.; Wei, Z.; Heidarinejad, M.; Dalgo, D.; Mi, R.; Zhao, X.; Song, J.; et al. A Radiative Cooling Structural Material. *Science* **2019**, *364* (6442), 760−763.
(181) Jia, C.; Chen, C.; Mi, R.; Li, T.; Dai, J.; Yang, Z.; Pei, Y.; He, S.; Bian, H.; Jang, S.-H.; Zhu, J. Y.; Yang, B.; Hu, L. Clear Wood toward High-Performance Building Materials. *ACS Nano* **2019**, *13* (9), 9993−10001.
(182) Li, T.; Zhang, X.; Lacey, S. D.; Mi, R.; Zhao, X.; Jiang, F.; Song, J.; Liu, Z.; Chen, G.; Dai, J.; Yao, Y.; Das, S.; Yang, R.; Briber, R. M.; Hu, L. Cellulose Ionic Conductors with High Differential Thermal Voltage for Low-Grade Heat Harvesting. *Nat. Mater.* **2019**, *18* (6), 608−613.
(183) Kong, W.; Wang, C.; Jia, C.; Kuang, Y.; Pastel, G.; Chen, C.; Chen, G.; He, S.; Huang, H.; Zhang, J.; Wang, S.; Hu, L. Muscle-Inspired Highly Anisotropic, Strong, Ion-Conductive Hydrogels. *Adv. Mater.* **2018**, *30* (39), e1801934.
(184) Song, J.; Chen, C.; Yang, Z.; Kuang, Y.; Li, T.; Li, Y.; Huang, H.; Kierzewski, I.; Liu, B.; He, S.; et al. Highly Compressible, Anisotropic Aerogel with Aligned Cellulose Nanofibers. *ACS Nano* **2018**, *12* (1), 140−147.
(185) Li, T.; Song, J.; Zhao, X.; Yang, Z.; Pastel, G.; Xu, S.; Jia, C.; Dai, J.; Chen, C.; Gong, A.; Jiang, F.; Yao, Y.; Fan, T.; Yang, B.; Wagberg, L.; Yang, R.; Hu, L. Anisotropic, Lightweight, Strong, and Super Thermally Insulating Nanowood with Naturally Aligned Nanocellulose. *Sci. Adv.* **2018**, *4* (3), eaar3724/1−eaar3724/9.
(186) Geng, S.; Wei, J.; Aitomäki, Y.; Noël, M.; Oksman, K. Well-Dispersed Cellulose Nanocrystals in Hydrophobic Polymers by *In Situ* Polymerization for Synthesizing Highly Reinforced Bio-Nanocomposites. *Nanoscale* **2018**, *10* (25), 11797−11807.
(187) Jonoobi, M.; Harun, J.; Mathew, A. P.; Oksman, K. Mechanical Properties of Cellulose Nanofiber (CNF) Reinforced Polylactic Acid (PLA) Prepared by Twin Screw Extrusion. *Compos. Sci. Technol.* **2010**, *70* (12), 1742−1747.
(188) Shrestha, S.; Chowdhury, R. A.; Toomey, M. D.; Betancourt, D.; Montes, F.; Youngblood, J. P. Surface Hydrophobization of TEMPO-Oxidized Cellulose Nanofibrils (CNFs) Using a Facile, Aqueous Modification Process and Its Effect on Properties of Epoxy Nanocomposites. *Cellulose* **2019**, *26* (18), 9631−9643.
(189) Uddin, A. J.; Araki, J.; Gotoh, Y. Toward "Strong" Green Nanocomposites: Polyvinyl Alcohol Reinforced with Extremely Oriented Cellulose Whiskers. *Biomacromolecules* **2011**, *12* (3), 617−624.
(190) Guo, W.; Cao, L.; Xia, J.; Nie, F. Q.; Ma, W.; Xue, J.; Song, Y.; Zhu, D.; Wang, Y.; Jiang, L. Energy Harvesting with Single-Ion-Selective Nanopores: A Concentration-Gradient-Driven Nanofluidic Power Source. *Adv. Funct. Mater.* **2010**, *20* (8), 1339−1344.
(191) Zhang, Z.; Sui, X.; Li, P.; Xie, G.; Kong, X.-Y.; Xiao, K.; Gao, L.; Wen, L.; Jiang, L. Ultrathin and Ion-Selective Janus Membranes for High-Performance Osmotic Energy Conversion. *J. Am. Chem. Soc.* **2017**, *139* (26), 8905−8914.
(192) Hou, X.; Jiang, L. Learning from Nature: Building Bio-Inspired Smart Nanochannels. *ACS Nano* **2009**, *3* (11), 3339−3342.
(193) Abraham, J.; Vasu, K. S.; Williams, C. D.; Gopinadhan, K.; Su, Y.; Cherian, C. T.; Dix, J.; Prestat, E.; Haigh, S. J.; Grigorieva, I. V.; Carbone, P.; Geim, A. K.; Nair, R. R. Tunable Sieving of Ions Using Graphene Oxide Membranes. *Nat. Nanotechnol.* **2017**, *12* (6), 546−550.
(194) Li, Y.; Li, X.; Cao, J.; Xu, W.; Zhang, H. Composite Porous Membranes with an Ultrathin Selective Layer for Vanadium Flow Batteries. *Chem. Commun.* **2014**, *50* (35), 4596−4599.
(195) Duan, C.; Wang, W.; Xie, Q. Fabrication of Nanofluidic Devices. *Biomicrofluidics* **2013**, *7* (2), 026501.


https://dx.doi.org/10.1021/acsnano.0c07613
*ACS Nano* 2021, 15, 3646−3673

(196) Li, T.; Li, S. X.; Kong, W.; Chen, C.; Hitz, E.; Jia, C.; Dai, J.; Zhang, X.; Briber, R.; Siwy, Z.; Reed, M.; Hu, L. A Nanofluidic Ion Regulation Membrane with Aligned Cellulose Nanofibers. *Sci. Adv.* **2019**, *5* (2), eaau4238.
(197) Zhou, Y.; Chen, C.; Zhang, X.; Liu, D.; Xu, L.; Dai, J.; Liou, S. C.; Wang, Y.; Li, C.; Xie, H.; Wu, Q.; Foster, B.; Li, T.; Briber, R. M.; Hu, L. Decoupling Ionic and Electronic Pathways in Low-Dimensional Hybrid Conductors. *J. Am. Chem. Soc.* **2019**, *141* (44), 17830−17837.
(198) Kuang, Y.; Chen, C.; Cheng, J.; Pastel, G.; Li, T.; Song, J.; Jiang, F.; Li, Y.; Zhang, Y.; Jang, S.-H.; Chen, G.; Li, T.; Hu, L. Selectively Aligned Cellulose Nanofibers towards High-Performance Soft Actuators. *Extreme Mech. Lett.* **2019**, *29*, 100463.
(199) Wang, S.; Zhang, X.; Wu, X.; Lu, C. Tailoring Percolating Conductive Networks of Natural Rubber Composites for Flexible Strain Sensors *via* a Cellulose Nanocrystal Templated Assembly. *Soft Matter* **2016**, *12* (3), 845−852.
(200) Cho, S.-Y.; Yu, H.; Choi, J.; Kang, H.; Park, S.; Jang, J.-S.; Hong, H.-J.; Kim, I.-D.; Lee, S.-K.; Jeong, H. S.; Jung, H.-T. Continuous Meter-Scale Synthesis of Weavable Tunicate Cellulose/Carbon Nanotube Fibers for High-Performance Wearable Sensors. *ACS Nano* **2019**, *13* (8), 9332−9341.
(201) Fu, W.; Dai, Y.; Meng, X.; Xu, W.; Zhou, J.; Liu, Z.; Lu, W.; Wang, S.; Huang, C.; Sun, Y. Electronic Textiles Based on Aligned Electrospun Belt-Like Cellulose Acetate Nanofibers and Graphene Sheets: Portable, Scalable and Eco-Friendly Strain Sensor. *Nanotechnology* **2019**, *30* (4), 045602.
(202) Shen, Y.; Orelma, H.; Sneck, A.; Kataja, K.; Salmela, J.; Qvintus, P.; Suurnäkki, A.; Harlin, A. High Velocity Dry Spinning of Nanofibrillated Cellulose (CNF) Filaments on an Adhesion Controlled Surface with Low Friction. *Cellulose* **2016**, *23* (6), 3393−3398.
(203) Petersen, N.; Gatenholm, P. Bacterial Cellulose-Based Materials and Medical Devices: Current State and Perspectives. *Appl. Microbiol. Biotechnol.* **2011**, *91* (5), 1277.
(204) Sultan, S.; Siqueira, G.; Zimmermann, T.; Mathew, A. P. 3D Printing of Nano-Cellulosic Biomaterials for Medical Applications. *Curr. Opin. Biomed. Eng.* **2017**, *2*, 29−34.
(205) Badrossamay, M. R.; McIlwee, H. A.; Goss, J. A.; Parker, K. K. Nanofiber Assembly by Rotary Jet-Spinning. *Nano Lett.* **2010**, *10* (6), 2257−2261.
(206) He, X.; Xiao, Q.; Lu, C.; Wang, Y.; Zhang, X.; Zhao, J.; Zhang, W.; Zhang, X.; Deng, Y. Uniaxially Aligned Electrospun All-Cellulose Nanocomposite Nanofibers Reinforced With Cellulose Nanocrystals: Scaffold for Tissue Engineering. *Biomacromolecules* **2014**, *15* (2), 618−627.
(207) Skogberg, A.; Maki, A.-J.; Mettanen, M.; Lahtinen, P.; Kallio, P. Cellulose Nanofiber Alignment Using Evaporation-Induced Droplet-Casting, and Cell Alignment on Aligned Nanocellulose Surfaces. *Biomacromolecules* **2017**, *18* (12), 3936−3953.
(208) Elashnikov, R.; Rimpelova, S.; Dekanovsky, L.; Svorcik, V.; Lyutakov, O. Polypyrrole-Coated Cellulose Nanofibers: Influence of Orientation, Coverage and Electrical Stimulation on SH-SY5Y Behavior. *J. Mater. Chem. B* **2019**, *7* (42), 6500−6507.
(209) Hua, K.; Rocha, I.; Zhang, P.; Gustafsson, S.; Ning, Y.; Stromme, M.; Mihranyan, A.; Ferraz, N. Transition from Bioinert to Bioactive Material by Tailoring the Biological Cell Response to Carboxylated Nanocellulose. *Biomacromolecules* **2016**, *17* (3), 1224−33.
(210) Hua, K.; Carlsson, D. O.; Ålander, E.; Lindström, T.; Strømme, M.; Mihranyan, A.; Ferraz, N. Translational Study between Structure and Biological Response of Nanocellulose from Wood and Green Algae. *RSC Adv.* **2014**, *4* (6), 2892−2903.
(211) Zou, J.; Wu, S.; Chen, J.; Lei, X.; Li, Q.; Yu, H.; Tang, S.; Ye, D. Highly Efficient and Environmentally Friendly Fabrication of Robust, Programmable, and Biocompatible Anisotropic, All-Cellulose, Wrinkle-Patterned Hydrogels for Cell Alignment. *Adv. Mater.* **2019**, *31* (46), 1904762.
(212) Gupta, S.; Martoïa, F.; Orgéas, L.; Dumont, P. J. J. Ice-Templated Porous Nanocellulose-Based Materials: Current Progress and Opportunities for Materials Engineering. *Appl. Sci.* **2018**, *8* (12), 2463.
(213) Flauder, S.; Heinze, T.; Mueller, F. A. Cellulose Scaffolds with an Aligned and Open Porosity Fabricated *via* Ice-Templating. *Cellulose* **2014**, *21* (1), 97−103.
(214) Li, G.; Nandgaonkar, A. G.; Habibi, Y.; Krause, W. E.; Wei, Q.; Lucia, L. A. An Environmentally Benign Approach to Achieving Vectorial Alignment and High Microporosity in Bacterial Cellulose/Chitosan Scaffolds. *RSC Adv.* **2017**, *7* (23), 13678−13688.
(215) Wang, X.; Wu, P. 3D Vertically Aligned BNNS Network with Long-Range Continuous Channels for Achieving a Highly Thermally Conductive Composite. *ACS Appl. Mater. Interfaces* **2019**, *11* (32), 28943−28952.
(216) Kumar, A. K.; Sharma, S. Recent Updates on Different Methods of Pretreatment of Lignocellulosic Feedstocks: A Review. *Bioresources and Bioprocessing* **2017**, *4* (1), 7.
(217) Wang, Q.; Sun, J.; Yao, Q.; Ji, C.; Liu, J.; Zhu, Q. 3D Printing with Cellulose Materials. *Cellulose* **2018**, *25* (8), 4275−4301.
(218) Compton, B. G.; Lewis, J. A. 3D-Printing of Lightweight Cellular Composites. *Adv. Mater.* **2014**, *26* (34), 5930−5.
(219) Wang, H.; Feng, Z.; Xu, B. Bioinspired Assembly of Small Molecules in Cell Milieu. *Chem. Soc. Rev.* **2017**, *46* (9), 2421−2436.
(220) Yao, H.-B.; Fang, H.-Y.; Wang, X.-H.; Yu, S.-H. Hierarchical Assembly of Micro-/Nano-Building Blocks: Bio-Inspired Rigid Structural Functional Materials. *Chem. Soc. Rev.* **2011**, *40* (7), 3764−3785.
(221) Dumanli, A. G.; Kamita, G.; Landman, J.; van der Kooij, H.; Glover, B. J.; Baumberg, J. J.; Steiner, U.; Vignolini, S. Controlled, Bio-Inspired Self-Assembly of Cellulose-Based Chiral Reflectors. *Adv. Opt. Mater.* **2014**, *2* (7), 646−650.
(222) Takana, H.; Guo, M. Numerical Simulation on Electrostatic Alignment Control of Cellulose Nano-Fibrils in Flow. *Nanotechnology* **2020**, *31* (20), 205602.
(223) Haakansson, K. M. O.; Lundell, F.; Prahl-Wittberg, L.; Soederberg, L. D. Nanofibril Alignment in Flow Focusing: Measurements and Calculations. *J. Phys. Chem. B* **2016**, *120* (27), 6674−6686.
(224) Nikolov, S.; Petrov, M.; Lymperakis, L.; Friák, M.; Sachs, C.; Fabritius, H.-O.; Raabe, D.; Neugebauer, J. Revealing the Design Principles of High-Performance Biological Composites Using *ab Initio* and Multiscale Simulations: The Example of Lobster Cuticle. *Adv. Mater.* **2010**, *22* (4), 519−526.
(225) Kurioz, Y.; Reznikov, Y.; Tereshchenko, O.; Gerus, I.; Buluy, O.; Ha, K. R.; Kim, D. H.; Kwon, S. B.; Park, S. K. Highly Sensitive Photoaligning Materials on a Base of Cellulose-Cinnamates. *Mol. Cryst. Liq. Cryst.* **2008**, *480*, 81−90.
(226) Yaroshchuk, O.; Reznikov, Y. Photoalignment of Liquid Crystals: Basics and Current Trends. *J. Mater. Chem.* **2012**, *22* (2), 286−300.


https://dx.doi.org/10.1021/acsnano.0c07613
*ACS Nano* 2021, 15, 3646−3673